Development, Characterization and in vivo Performance Analysis of Doped Beta- Tricalcium phosphate Ceramics

Thesis Submitted

By

Sujan Krishna Samanta

Doctor of Philosophy (Engineering)

SCHOOL OF BIO-SCIENCE & ENGINEERING
FACULTY COUNCIL OF ENGINEERING & TECHNOLOGY
JADAVPUR UNIVERSITY
KOLKATA, INDIA
2019

JADAVPUR UNIVERSITY
KOLKATA-700032, INDIA

INDEX NO. 283/12/E

1. Title of the thesis:

"Development, characterization and in vivo performance analysis of doped Beta tricalcium phosphate ceramics"

2. Name, Designation & Institution of Supervisor/s:

Dr. Abhijit Chanda

Professor

Department of Mechanical Engineering

Jadavpur University

Kolkata-700032

&

Dr. Samit Kumar Nandi

Professor

Department of Veterinary Surgery & Radiology

West Bengal University of Animal and Fishery Science

Kolkata-700037

CERTIFICATE FROM THE SUPERVISOR/S

This is to certify that the thesis entitled **"Development, characterization and in vivo performance analysis of doped Beta-tricalcium phosphate ceramics"** submitted by Sujan Krishna Samanta, who got his name registered on 13/03/2012 for the award of **Ph.D.(Engineering) degree** of **Jadavpur University**, is absolutely based upon his own work under the supervision of **Dr. Abhijit Chanda and Dr. Samit Kumar Nandi,** and that neither his thesis nor any part of the same has been submitted for any degree / diploma or any other academic award anywhere before.

Dr. Abhijit Chanda

Professor
Department of Mechanical Engineering
Jadavpur University
Kolkata-700032

Dr. Samit Kumar Nandi

Professor
Department of Veterinary Surgery
& Radiology,West Bengal
University of Animal and Fishery
Science, Kolkata-700037

DEDICATION

To my Father Late Bata Krishna Samanta and to my mother Santilata Samanta for all your love, patience, and encouragement over the years.

To my supervisor Dr. Abhijit Chanda, without you I would not be where I am today. Thank you for always being only a phone call away!

To my wife Smitisha, for all your love and support. You always manage to bring a smile to my face. Thank you for sharing this journey with me!

PREFACE

This thesis is the result of my own work and includes nothing which is the outcome of work done in collaboration, except where specifically indicated in the text and acknowledgements. The research was conducted primarily at the School of Bio-Science and Engineering, Jadavpur University and also at the laboratories of West Bengal university of animal and Fishery Science, Kolkata and Central Research Facility, IIT-Kharagpur during the years from 2012 to 2018, under the supervision of Dr. Abhijit Chanda of Dept. of Mechanical Engineering, Jadavpur University and Dr. Samit Kumar Nandi, Department of Veterinary Surgery & Radiology, West Bengal University of Animal and Fishery Science, Kolkata.

No part of this thesis has already been or is being concurrently submitted for any degree, diploma or other qualification.

Acknowledgement

First and foremost I would like to express my deepest regards and respect to the most important person of my thesis advisor ***Dr. Abhijit Chanda, Dept. of Mechanical Engineering, Jadavpur University,*** for his esteemed guidance, invaluable suggestions, constant encouragement and affection at every stage of my work. He has not only been my guide but more like a friend to me. Without him conceiving this study would have been impossible. My heart will always bear respectful gratitude to him.

My deepest gratitude goes to my co-guide ***Dr. Samit Kumar Nandi, Department of Veterinary Surgery & Radiology, West Bengal University of Animal & Fishery Science, Kolkata***. I am very grateful for his tremendous help and kind support behind this research. He has educated me on different aspects of animal trials. The thesis work would never be possible without his help.

I express my gratefulness to ***Director, Piyali Basak, School of Bio Science & Engineering****, Jadavpur University, Kolkata and* ***Honorable Vice Chancellor, West Bengal University of Animal and Fishery Sciences*** *for providing me the facilities to do this research work. I express my indebt ness to* ***Director, Netaji Subhash Engineering College and Techno India Group*** *for giving me opportunities to go with this work.*

During my research, ***Dr. Biswanath Kundu, CGCRI, Kolkata*** helped me a lot for sample preparation. I would like to give my sincere thanks to Dr.Kundu for his kind help.I offer my cordial thanks to ***Dr. Anoop Kumar Mukhopadhyay, CGCRI Kolkata***, for providing all the necessary help and technical support during my work. I would like to express my appreciation to Dr. ***Dr. Mangal Roy and K. Bavya Devi, Department of Metallurgical and Materials Engineering, IIT, Kharagpur****, India for extending their help in material characterization and in vivo studies.*

I also like to express my special gratitude to ***Anupam Maiti of Biomedical Engg Dept.,NSEC*** *for his kind help* ***and Tapash Dawn of NSEC*** *for his support to develop the machine for this work..*

I would like to acknowledge ***Howa, Pranabesh, Sourav, Sarmita, Somali, Akash and Bablu*** for being more like a family member to me during my entire research work. Last but certainly not the least, I would like to thank my ***mother, wife*** and all other family members for their immense support and constant enthusiasm whenever I tried to tread a lesser walked lane. Without their help I could have never achieved anything in any sphere of life.

March, 2019

(Sujan Krishna Samanta)
School of Bio-Science & Engineering, JU

TABLE OF CONTENTS

Preface	v
Acknowledgement	vi
Abstract	vii
Table of contents	viii
List of tables	ix
List of figures	x-xi
Abbreviation	xii-xiii
List of publications	xiv
Introduction	1-10
Literature survey	11-30
Scope of the work & objective	31-32
Materials and method	33-49
Results & discussion	50-84
Conclusion & future scope	85-86

LIST OF TABLES

SL. NO.	TABLE NAME	PAGE NO.
Table 1.1:	Physical property of various phases of calcium phosphates ceramics	2
Table 1.2:	Classification of different bioceramics	3
Table 4.1:	Ion concentration of SBF in comparison with human blood plasma	40
Table 4.2:	Reagents for preparation of SBF	41
Table 5.1:	Result of Lattice parameters	52
Table 5.2:	Green density of pure β- TCP and its derivatives	54
Table 5.3:	Percentage of diametric, linear and volumetric shrinkage at different temperatures	56
Table 5.4:	Apparent porosity at different temperatures	58
Table 5.5:	Grain Size and pore size	59
Table 5.6:	Contact angle study results	60
Table 5.7:	Hardness value	62
Table 5.8:	Hemolysis observation data for all compositions	65
Table 5.9:	Data for hemolysis analysis.	65
Table 5.10:	Oxytetracycline labelling study result	78

LIST OF FIGURES

SL. NO.	NAME OF THE FIGURE	PAGE NO.
Figure 4.1	Steps of creating bone defect and implantation.	45
Figure 4.1	The machine which was used to produce axial oscillatory vibration. A. Inside B. Outside	46
Figure 5.1	XRD pattern of pure β-TCP	51
Figure 5.2	XRD pattern of β-TCP along with its doped Variants	52
Figure 5.3	FTIR spectra of pure β-TCP	53
Figure 5.4	FTIR spectra of β-TCP along with its doped Variants	54
Figure 5.5	The average green density of all compositions	55
Figure 5.6	Bar diagram of apparent porosity at different temperatures	59
Figure 5.7	SEM images of pure β- TCP at different magnification (a) 5000X,(b)8000X, (c) 10000X, (d) 12000X	61
Figure 5.8	SEM images of doped samples: (a) 3%Zn-β- TCP , (b) 3% Mg-β-TCP, (c) 3% Ti- β-TCP, (d) 5% Zn- β-TCP, (e) 5% Mg-β-TCP, (f) 5% Ti-β-TCP	61
Figure 5.9	EDS pattern of pure and 5 % doped β-TCP, sintered at 1100° C(a) Pure β-TCP (b) Zn-β-TCP (c) Mg -β-TCP (d) Ti -β-TCP	62
Figure 5.10	SEM images of apatite: (a) β- TCP , (b) 3%Zn-β- TCP , (c) 3% Mg-β-TCP, (d) 3% Ti- β-TCP, (e) 5% Zn- β-TCP, (f) 5% Mg-β-TCP, (g) 5% Ti- β-TCP	63
Figure 5.11	Plot of percentage weight degradation in SBF with days	64
Figure 5.12	Plot of transmittance percentage of β-TCP and its dopants of SBF solution	64
Figure 5.13	Bar diagram of % Hemolysis	66

Figure 5.14	% cell viability as observed in MTT assay	66
Figure 5.15	Petridish images	67
Figure 5.16	Radiographs of the '0' day	70
Figure 5.17	Radiographs of the '30' day	71
Figure 5.18	Radiographs of the '60' day	72
Figure 5.19	Radiographic 2D images of defect bone sites; with control: (A) 30 Days. (B) 60 Days. With β- TCP : (C) 30 Days. (D) 60 Days, with Ti -β-TCP: (E) 30 Days. (F) 60 Days	72
Figure 5.20	3D micrographs of defect bone sites; with control: (A) 30 Days. (B) 60 Days. With β-TCP: (C) 30 Days. (D) 60 Days, with Ti- β-TCP: (E) 30 Days. (F) 60 Days	73
Figure 5.21	Radiographic 2D images of group III animal;1 M after installation: A. β-TCP, B. Zn- β-TCP, C. Mg- β-TCP, D. Ti- β-TCP and 2 M after installation: E. β-TCP, F. Zn- β-TCP, G. Mg- β-TCP, H. Ti- β-TCP	73
Figure 5.22	Radiographic 3D images of group III animal: 1 M after installation. A.β-TCP, B. Zn- β-TCP, C. Mg- β-TCP, D. Ti- β-TCP and 2 M after installation. E. β-TCP, F. Zn- β-TCP, G. Mg- β-TCP, H. Ti- β-TCP	74
Figure 5.23	Histological section of the bone of control & Gr. II animal after 1 M: (A) Control (B) β-TCP (C) Ti- β-TCP, after 2 M: (D) control (E) β- TCP (F) Ti- β-TCP	75
Figure 5.24	Histological section of the bone in group III after 1M of installation.A. β-TCP, B.Zn- β-TCP, C. Mg- β-TCP, D.Ti- β-TCP and after 2M of installation. E. β-TCP, F. Zn- β-TCP,G.Mg- β-TCP, H.Ti- β-TCP	76
Figure 5.25	Oxytetracycline labeling study at the defected site of the group Control, Group II & Group III animal after 1M and 2M of installation.	78
Figure 5.26	Bar diagram showing % new bone formation in 1 month and 2 Month	78
Figure 5.27	SEM images of all groups of bone implant interface after 1 Month & 2 Month	79

LIST OF ABBREVIATIONS

TCP	Tri Calcium Phosphate
HAP	Hydroxyapatite
ASTM	American Society for Testing and Materials
MN	Mononuclear Cell
TTCP	Tetra Calcium Phosphate
Ca-P	Calcium Phosphate
SEM	Scanning Electron Microscope
FTIR	Fourier Transform Infrared Spectroscopy
GPa	Giga Pascal
BMP	Bone Morphogenetic Protein
TGF	Transforming Growth Factor
JCPDS	Joint Committee On Powder Diffraction Standards
OD	Optical Density
OTC	Oxy-tetracycline dihydrate
SBF	Simulated Body Fluid
NV	No vibration
WV	With vibration

β-TCP	Beta tri calcium phosphate
SD	Standard Deviation
1M	One Month
2M	Two Month
XRD	X-Ray Diffraction
PBMC	Peripheral Blood Mononuclear Cell
HC	Haversian Canal
BII	Bone-Implant-Interfaces
SGPs	Strain Generated Potentials
WBV	whole-body vibration
LIV	Low Intensity Vibration

LIST OF PUBLICATIONS

Journal publications

1. Sujan Krishna Samanta and Abhijit Chanda , Study on different characteristics of doped tri calcium phosphate at different sintering temperatures, AIP Publishing 1724, 020042,2016
2. Sujan Krishna Samanta, Abhijit Chanda ,Study on the Structure and Properties of Crystalline Pure and Doped β-Tri Calcium Phosphate Ceramics, Materials Today: Proceedings 5 , 2330–2338m,2018
3. Sujan Krishna Samanta, Abhijit Chanda and Samit Kumar Nandi, Physical and Mechanical Characterization of Crystalline Pure β-Tri Calcium Phosphate & Its Dopants as Bone Substitutes, accepted in, IOP Science ,2018.
4. Sujan Krishna Samanta, K. Bavya Devi,Piyali Das, Prasenjit Mukherjee, Abhijit Chanda, Mangal Roy and Samit Kumar Nandi, Metallic Ion Doped Tri-calcium Phosphate Ceramics: Effect of Dynamic Loading on in vivo Bone Regeneration, Journal of the Mechanical Behavior of Biomedical Materials 96, 227–235. 2019

List of patents: Nil

List of presentations in national/international

1. Study on different characteristics of doped tri calcium phosphate at different sintering Temperatures, 2nd International Conference on Emerging Technologies: Micro to Nano,October 24-25th 2015, Manipal University Jaipur, Rajasthan.

2. Study on the structure and properties of crystalline pure and doped beta-tri calcium phosphate ceramics, 2nd International Conference, 16-18th February, ICMS-2017, Tripura.

3. In vitro characterization of crystalline pure β-tri calcium phosphate and its dopants as bone substitute, International Conference on Advances in Materials and Manufacturing Applications. Amrita Vishwa Vidyapeetham, Bangalore, August 16th-18th,2018

CHAPTER: 1

INTRODUCTION

1.1 Introduction

With increasing life expectancy world over (being 65 years in India and 75+ years in western countries) bone and Joint associated problems and fracture due to trauma and aging are becoming common. This is true in orthopedics as well as in dental surgery. Biomaterials as calcium phosphate ceramics have been accepted as the most suitable biomaterial for bone and teeth replacement due to their elemental and biotic similarity with the constituents of human hard tissue [1]. On application, the bioactive materials like Calcium phosphate ceramics encourage specific tissue reaction which consequences in the development of a connecting interface among the inserted material with the regular bone tissue. Calcium phosphate based biomaterials are mainly utilized as osteo-conductive material for artificial bone graft, drug carrier and coating on metallic implants or on different prosthesis (in hip prosthesis and dental implants).Today Calcium phosphate-based ceramic materials have also found wide spread uses as bioresorbable materials . Among commonly used calcium phosphates, β-Tri calcium phosphate (β-TCP) and hydroxyapatite phosphate (HAP) are the most regularly used composition. Due to its time-bound mechanical and dissolution characteristics and excellent osteoconductive properties, β-Tri calcium phosphate has been extensively used as bone cement and as implant material. In numerous applications, the time-dependent resorption characteristics make β-TCP a perfect material for implantation; this ceramic can supply short-term support for bone in growth, and is eventually displaced by natural tissue.

There are three allotropic forms, α, α′ and β in tricalcium phosphate among which β-TCP has been found to be the most attractive in terms of chemical steadiness and bioresorption rate. The dissolution profile of β-TCP is much faster than HAP, the other mostly used Ca-phosphate based ceramic.

Due to its outstanding biocompatibility and super bioactivity, β-TCP is more popular than HAP for the restoration of certain orthopedic applications, for periodontal defects, and maxillofacial surgery. Ca/P ratio is very important for degradability of these compounds. HAP having the Ca/P ratio 1.667 is firmly stable in body fluid and takes much time, even some years to be resorbed. On the other hand β-TCP is having a Ca/P ratio of 1.5, which makes it biodegradable and, can be completely replaced by newly formed bone after implantation.

Physical properties of various phases of calcium phosphates ceramics [2, 3] are given in table1.1.

Table 1.1: Physical property of various phases of calcium phosphates ceramics

Phases	**Chemical Formula**	**Ca/P ratio**	**Density (gm/cc)**	**Solubility at 37°C (mgL^{-1})**	**Crystal Structure**
β-tricalcium phosphate	$Ca_3(PO4)_2$	3/2	3.066	0.15	Pure hexagonal, rhombohedral, space group R3Ch,unit cell dimension:a=b=10.439A°, c=37.375A°,and α=β=90°, γ=120°
α-tricalcium phosphate	$Ca_3(PO4)_2$	3/2	2.866	0.24	Monoclinic,$P2_1/a$ space group, lattice constants: a=12.887A°, b=27.280A°,c=15.219A°; β=126.20°
Hydroxy apatite	$Ca_{10}(PO_4)_6(OH)_2$	10/6	3.167	9.6×10^{-5}	Hexagonal,$P6_3/m$ space group, cell dimension : a=b=9.42A° and c=6.88A°
Tetra calcium phosphate	$Ca_4P_2O_9$	2/1	3.05	0.39-0.075	Monoclinic, space group $P2_1/a$=7.023 A°, b=11.986 A°, c=9.473 A°, β=90.90 °

1.2 Bioceramic: Ceramics applied for the healing and restoration of diseased or damaged body parts or wounds are called bioceramic. These compounds are biocompatible. They constitute a chief subset of biomaterials [4]. Bioceramics are used in many different types of medical procedures. A primary medical procedure where they are used is as implants. They are anticorrosive; this makes bioceramics suitable for medical usage. Alumina, Zirconia ceramic have bio-inertness and non-cytotoxicity. Carbon with parallel mechanical properties of bone is also an alternative, for its blood compatibility and nontoxicity nature to cells. The bioinert ceramics can be made bioactive by forming composites with bioactive ceramics. Bioglass and glass ceramics are safe, non toxic and they chemically bond with bone. Glass ceramics elicit osteoinductive property. Inert bioceramics are often used for load bearing bone and joint surgery

where predominantly compressive stress acts. Bioactive glass and phosphate based ceramics are applied as bone and dental fillers. They are also used as surface coating on metallic implants. Owing to inherent brittleness, bioceramic materials find limited use as bulk components, wide use as granules, powders, and coating materials. Different kind of bioceramics are presented in below table no 1.2.

Table 1.2: Classification of different bioceramics

Type	**Example**	**Type of attachment**
Bioinert	Zirconia, Alumina	Dense, non- porous nearly inert ceramics, join by bone growth into surface irregularities by cementing the devices into the tissues or by press – fitting into a defect (morphological fixation)
Bioactive	Bioactive glass ceramics, Bioactive glasses, HAP	Nonporous, dense, surface reactive ceramics, glasses and glass ceramics join directly by chemical bonding with the bone (Bioactive fixation)
Bioresorbable	Tri calcium phosphate, calcium phosphate salts, Plaster of paris	Dense, non porus or porus, resorbable and slowly replaced by bone cells.

One newly projected application area for bioceramic is in the management of cancer [5]. Two methods of management have been recommended. These are healing through hyperthermia and through radiation therapy. Treatment by Hyperthermia includes planting a bioceramic material that contains magnetic material like ferrite or others and subsequently exposed to alternating magnetic field to heat up. In other way, the bioceramic substances can be doped with β-emitting materials and embedded into the cancerous area.

1.3 Doping and Doped bioceramic:

Production of ion-substituted (metal ion) calcium phosphates has attracted ample research concern as metal ion replacement has been revealed to enhance the mechanical characteristics and higher bioactivity of grafts. Plenty of literatures are available where addition of dopants such as Zn/Mg/Ti/Ca/Si/Na and Ag influence the mechanical characteristics of β-TCP without changing its integral biocompatibility. Researchers have also established that ZnO doping increases the densification of β-TCP ceramics [6]. Addition of Mg and Ti ions in calcium phosphate ceramic is of huge interest as these ions show a significant role in new bone development. The need for zinc in human body is small, but its function in growth and well-being is enormous, primarily even before birth. In vitro studies confirm that Zn has direct definite proliferative effect on osteoblastic cells [7] and a strong and selective inhibitory consequence on osteoclastic bone resorption [8]. In vivo results on Zn doped calcium phosphates ceramics on rabbit femora showed over 50% more newly formed bone over 0% Zn calcium phosphate composition. Recent research outcomes also linked clinical relationship between osteoporosis and Zn insufficiency in elder persons. Zinc doping calcium phosphate has influenced the prompt new bone formation [9]. Recently, in vitro and in vivo research works have undoubtedly specified the useful effects of Titanium on bone development. It has been suggested that titanium's role for osseointegration derives from the high dielectric constant of its surface oxide, which does not denature proteins [10]. High surface energy of titanium enables it to induce angiogenesis, which supports in the process of osseointegration. Mg is also certainly one of the most significant bivalent ions related with biological apatites. Replacement of Mg in calcium phosphate ceramics has received plenty scientific concerns due to its potential role in qualitative changes in bone environment, and its secondary influence on mineral uptake, encouraging catalytic reactions and governing biological functions. Magnesium shortage contributes to osteoporosis directly by acting on crystal development and on bone cells and indirectly by influencing on the secretion and the activity of parathyroid hormone and by promoting low grade inflammation [11].

1.4 Bone healing and the effects of dynamic loading:

Bone healing is a proliferative physiological procedure in which the body aids the restoration of a bone fracture or rupture. The healing procedure will depend on the nature and amount of the damage, the stability of fracture fixation, and biological processes, so a proper healing development is very crucial.

There are three primary stages of bone healing: 1. Primary inflammatory phase 2. Repair phase 3.The late remodeling phase [12].

1. The Primary inflammatory phase - This starts immediately after bone damage or injury with the development of a local hematoma or fibrin clot. There is local cell death where vessel distraction has resulted in ischemia - usually at the very ends of the cracked bone. Over the way of the subsequent few days, this area becomes infiltrated by inflammatory cells and is characterized by local inflammation and warmth. The inflammatory cells discharge lysosomal enzymes and other mediators that draw pluripotent cells to the region; they also perform to eliminate necrotic tissue. Mesenchymal cells, osteoprogenitor cells and fibroblasts come into the region and may change to nearby tissues. The breakage is tender and may be grossly movable to physical examination at this phase. Inflammation is at its peak at 48 hours after a break.

2. Repair phase –This stage starts a few days later the injury with the appearance of mesenchymal cells able to differentiate into osteoblast, chondroblasts and fibroblasts. The repair stage continues for more than a few months; it can be separated into two distinct segment: soft and hard callus development.

i. "Soft callus" development precedes for roughly six weeks from the time of bone damage. During this preliminary phase of restoration, pain and inflammation subside and bony fragments become united by fibrous and cartilaginous tissue. Woven bone is created. While this creates some stability, the fracture may still angulated at this stage if not held with firm outside support, such as external fixator or a cast or, or internal support provided by screws, plates or intramedullary devices.
ii. "Hard callus" development - Throughout this second phase of repair, woven bone is changed into lamellar bone. This takes about three months.

3. Remodeling stage - Remodeling is the course of development by which bone is removed in minute increments and then displaced by fresh bone following a bone damage or fracture. Remodeling may prolong for months or even years. The mature human skeleton constantly replaces itself at a rate of 10-18% per year. The speed of remodeling goes faster in children and during fracture repair. In adding to being a crucial part of fracture healing, remodeling does a significant job in calcium homeostasis. During the remodeling stage the woven bone is transformed to lamellar bone and the medullary canal is reconstructered. During this stage, bone responds to loading characteristics according to Wolff's law.

There are many processes studied by the researchers to make the bone healing process quicker. This bone healing process can be made faster by the application of different bone substitute like β- tri calcium phosphate and its different derivatives. Many researchers have proved that mechanical stimulants are important factors for faster bone healing [13]. Application of vibration has been considered comprehensively for its effects on humans at specific frequencies and amplitudes [14].

Mechanical loads are potent factors in bone biology, affecting bone tissue morphology, development, repair and aging [13]. Shortage of physical activity causes bone damage, bone loss and ruptures not only in aged people, but also in inactive youth and in bedridden patients. This is rapidly becoming one of the most severe healthcare problems in the world. Osteocytes, cells submerged within our bones, excite bone development in the presence of mechanical stimulus, as well as bone degradation in the lack of such stimulus [14].

Physical movement with and without outside load is significant for preserving bone mass [15]. Less activity is one of the key explanations for the slow loss of bone mass in elderly stage. Low-amplitude, high frequency whole-body vibration (WBV) has been suggested as a management for osteoporosis, since scientific reports have showed that WBV can encourage the development of fresh trabecular bone. Though, the methods by which vibrational loading encourage bone development are not known [16].The actual mechanism of action behind healing due to vibration is not yet fully understood; however, numerous concepts have been proposed so far [17].

1. In the management of bone density, many investigators claim that mechanical vibration provides substantial but harmless stress on the patient's bones. The stress produced by the vibration guides an unidentified bio-chemical signal to the bones. This signal may guide the bones to enhance their internal mass.

2. According to another theory, mechanical stimulus reasons for stimulation of the musculature ensuing in mechanotransduction of strains inside bone, imitating mechanical signals typically created by postural muscle contractions or low intensity actions like as walking [18, 19 and 20].

3. One more suggestion is that mechanical stimulatory signals are amplified within the bone tissue by stress-generated increase in fluid flow causing from straight forward bone stimulation, thereby triggering osteocytes, which performs as mechanosensors to precede the skeleton's response [21,22].

4. On the other hand, there is also substantial confirmation that proposes the vibrations cause larger movements of cell nuclei than fluid-shear, signifying the method of action is more likely due to the mechanical union between these swing cell nuclei and the cytoskeleton, which eventually encourages actins remodeling and decreases bone resorption.

5. Osteocytes are the cells which encompasses over 90 % of the bone cells. Osteocytes are satellite cells that are inserted within the calcified bone matrix. They construct a large number of cell-cell contacts. [23] Osteocytes are reported to be extremely mechanosensitive, likely more so than periosteal fibroblasts or osteoblasts, and change the production of a multitude of signaling molecules when prompted by a mechanical stimulus. These cells are likely to be responsible for detecting the physical stimuli resulting from mechanical forces applied on bone.. Mechanically triggered osteocytes yield signaling molecules like bone prostaglandin E2 (PGE2),morphogenetic proteins (BMPs), and NO, which can modulate the differentiation, recruitment, and activity of osteoblasts and osteoclasts Robling et al., [24]; Tan et al., [25]; You et al., [26]; Santos et al., [27] . Thus, osteocytes are hypothetically skilled of orchestrating bone adaptation in reply to mechanical stimuli. Joel Edion we J et al [28] studied on outcome of whole-body vibration exercise on bone mineral content and density in thermally wounded children .They concluded that children getting better from burns, use of exercise in combination with WBV is an well accepted proposition. Yunita Sari et al [29] performed a comparison of the effects of vibration and electrical stimulation therapies on the speedy wound healing process in diabetic ulcers, and concluded that wound healing in diabetic ulcers by vibration was better than electrical stimulation. Da Jing et al., [30] concluded that porous titanium implants accompanied by Whole Body Vibration stimulation show high effectiveness and quality in the restoration of long bone defects, and also anticipated that vibration may eventually become a clinically pertinent management modality for osseous defects.

To summarise, it may be stated that number of hypotheses have been put forward to explain the effect of dynamic loading on bone remodeling but the results still vary a lot. Moreover all the possible variables as far as vibration is concerned are not yet studied. The main focus of the present stems out from the limitations of these research papers.

References

[1]. X. V. BÙI, Synthesis and in vitro Experiment of Biomaterial Tricalcium Phosphate, Asean J. Sci. Technol. Dev., 33(2): 78 – 84,2016.

[2].K. De Groot, C.P.A.T. Klein, J.G.C. Wolke, J.M.A. Blieck-Hogervorst, Chemistry of calcium phosphate bioceramics, CRC Handbook of Bioactive Ceramics, . Calcium Phosphate and Hydroxylapatite Ceramics, vol. II, CRC press, Boca Raton, FL, 1990.

[3].W.G. Billottee, in: J.B. Park, J.D. Bronzino (Eds.), Ceramic Materials in "Biomaterials: Principles and Applications", CRC Press, Boca Raton, FL, 2002.

[4].J. F.Shackelford (editor) MSF bioceramics applications of ceramic and glass materials in medicine ISBN 0-87849-822-2, 1999.

[5].Vallet-Regí, M., & Ruiz-Hernández, E. Bioceramics: From Bone Regeneration to Cancer Nanomedicine. Advanced Materials, 23(44), 5177–5218, 2011.

[6].Feng, P, Wei P, Shuai, C, & Peng, S. Characterization of Mechanical and Biological Properties of 3-D Scaffolds Reinforced with Zinc Oxide for Bone Tissue Engineering. PLoS ONE, 9(1), e87755, 2014.

[7].M. Hashizume, M. Yamaguchi, Mol. Cell. Biochem. 122 59, 1993.

[8].S. Kishi, M. Yamaguchi, Biochem. Pharmacol. 48 1225, 1994.

[9].P.Bhattacharjee, H. Begam, A. Chanda, S.K.Nandi, Animal trial on zinc doped hydroxyapatite: A case study, Journal of Asian Ceramic Societies 2 44–51, 2014.

[10].Black J, Biological performance of tantalum. Clin Mater 16: 167–173, 1994.

[11].Castiglioni, S., Cazzaniga, A., Albisetti, W., & Maier, J. Magnesium and Osteoporosis: Current State of Knowledge and Future Research Directions. Nutrients, 5(8), 3022–3033, 2013.

[12].Kalfas, I. H. Principles of bone healing. Neurosurgical Focus, 10(4), 1–4, 2001.

[13]. M Cardinale1, J Wakeling Whole body vibration exercise: are vibrations good for you? British Journal of Sports Medicine, Volume 39, Issue 2005; 39:585–589.2005

[14]. J. Klein-Nulend, R.G. Bacabac ,A.D. Bakker Mechanical Loading and How It Affects Bone Cells: The Role Of The Osteocyte Cytoskeleton In Maintaining Our Skeleton ,European Cells & Materials,24,278-291,2012.

[15].LeBlanc A, Schneider V, Krebs J, Evans H, Jhingran S, et al. Spinal bone mineral after 5 weeks of bed rest. Calcif Tissue Int 41: 259-261. 1987.

[16].Constrained tibial vibration does not produce an anabolic bone response in adult mice Blaine A. Christiansen , Akhilesh A. Kotiya, Matthew J. Silva, Bone 45 750–759,2009

[17].Rajapakse Chamith S, Leonard Mary B, Kobe Elizabeth A, Slinger Michelle A, Borges Kelly A, Billig Erica. Rubin, Clinton T, Wehrli Felix W, The Efficacy of Low-intensity Vibration to Improve Bone Health in Patients with End-stage Renal Disease Is Highly Dependent on Compliance and Muscle Response. Academic Radiology. June 2017

[18].Rubin C, Turner AS, Bain S, et al. Anabolism. Low mechanical signals strengthen long bones. Nature , 412:603–604.2001.

[19].Judex S, Rubin CT. Is bone formation induced by high-frequency mechanical signals modulated by muscle activity? J Musculoskelet Neuronal Interact, 10:3–11,2010.

[20].Ozcivici E, Luu YK, Adler B, et al. Mechanical signals as anabolic agents in bone. Nat Rev Rheumatol, 6:50–59. 2010.

[21].Cheung JTM, Zhang M, Chow DHK. Biomechanical responses of the intervertebral joints to static and vibrational loading: a finite element study. ClinBiomech (Bristol, Avon), 18:790–799, 2003.

[22].Stewart JM, Karman C, Montgomery LD, et al. Plantar vibration improves leg fluid flow in perimenopausal women. Am J PhysiolRegulIntegr Comp Physiol ,288:R623–R629,2005.

[23].Klein-Nulend J, Bacabac R.G. and Bakker A.D. Mechanical Loading And How It Affects Bone Cells: The Role Of The Osteocyte Cytoskeleton In Maintaining Our Skeleton. European Cells and Materials 24, 278-291, 2012.

[24].Robling Alexander G, Castillo Alesha B., and Turner Charles H., Biomechanical and Molecular Regulation of Bone Remodeling,Annu. Rev. Biomed. Eng, 8:455–98,2006.

[25].Tan SD, de Vries TJ, Kuijpers-Jagtman AM, Semeins CM, Everts V, Klein-Nulend J Osteocytes subjected to fluid flow inhibit osteoclast formation and bone resorption, Bone 41: 745-751, 2007.

[26].You L, Temiyasathit S, Lee P, Kim CH, Tummala P, Yao W, Kingery W, Malone AM, Kwon RY, Jacobs CR Osteocytes as mechanosensors in the inhibition of bone resorption due to mechanical loading. Bone 42: 172-179, 2008.

[27].Santos A, Bakker AD, Zandieh-Doulabi B, Semeins CM, Klein-Nulend J Pulsating fluid flow modulates gene expression of proteins involved in Wnt signaling pathways in osteocytes. J Orthop Res 27: 1280-1287, 2009.

[28]. Edionwe J, Hess C, Fernandez-Rio J, Herndon D N,. Andersen C R , Klein G L , Suman O E, Amonette W E, Effects of whole-body vibration exercise on bone mineral content and density in thermally injured children B u r n s 4 2 6 0 5 – 6 1 3, 2 0 1 6 .

[29].Sari Y, Saryono S, Sutrisna E, Hartono H, A comparative study of the effects of vibration and electrical stimulation therapies on the acceleration of wound healing in diabetic ulcers, Jurnal Ners , Vol. 12 No : 253-260,2017

[30]. Jing Da, Tong S, Zhai M , Li X, Cai J, Wu Y, Shen G, Zhang X, Xu Q, Guo Z & Luo E. Effect of low-level mechanical vibration on osteogenesis and osseointegration of porous titanium implants in the repair of long bone defects, Scientific Reports 5:17134

CHAPTER: 2

LITERATURE REVIEW

Introduction

Calcium phosphate (CaP) is the common name of a class of minerals having calcium cations (Ca^{2+}) along with orthophosphate (PO_4^{3-}), metaphosphate (PO_3^-), or pyrophosphate ($P_2O_7^{4-}$) anions, and sometimes hydrogen (H^+) or hydroxide (OH^-) ions. It is the chief inorganic component of bone (~60 wt % of bone), and the main integral material of tooth enamel. Calcium phosphates with a Ca/P atomic ratio between 1.5 and 1.67 are called apatites (e.g., hydroxyapatite or fluorapatite). In 1786 the term "apatite" was created by German geologist Abraham Gottlob Werner based on the ancient Greek word "apatao", which means "to mislead".

In the year 1920, Albee *et al.* [1] did the first successful application of a calcium phosphate reagent i.e triple calcium phosphate for restoring bone defect in human. More than five decades later, clinical use of a "tricalciumphosphate" in surgically produced periodontal defects in animal was described by Nery *et al.*[2] .The role of dense hydroxyapatite (HAP) as immediate tooth root replacements was informed by Dennissen *et al.* [3].In the early 1980s, artificially developed HAP and β- tricalcium phosphate (β-TCP) ,became commercially presented as bone substitute materials for dental medical applications largely through the huge efforts of Jarcho *et al.* and other researchers [4-6].

2.1 Synthesis of β-TCP

Several different synthesis methods for calcium phosphate based ceramics have been established since many years ago. These procedures include solid state reaction by Pramanik *et al.* [7], wet chemical method, hydrothermal synthesis by Liu *et al.*[8], and Kwon *et al.*[9], sol-gel procedures, mechanochemical synthesis by Yeong *et al.*[10], electrochemical deposition, microwave irradiation by Kumar *et al.* [11], and Xinlong Wang *et al.*[12] and combustion synthesis by Tas *et al* [13]. A chemical precipitation process is suggested in order to obtain nanosize β-TCP powders at low temperature by Bow *et al.*[14]. Many researchers used different natural compounds like egg shell, coral, fish to prepare it [15].

Siddharthan *et al.*[16] accelerated the development of calcium deficient hydroxy apatite (CDHA) by using microwaves in a less processing time at 650°C. In recent past, much work has been done towards the development of advanced processing techniques for achieving more functionally reliable bioceramic bodies. Refinement of grains, advancement in sintering process through microwave, doping with various ions are some of the approaches adopted for improving different characteristics of bio-ceramic material.

M. Jarcho *et al.*[17] described a novel process for preparing dense, polycrystalline tricalcium phosphates. Kaili Lin *et al.* [18] prepared β-$Ca_3(PO_4)_2$bioceramics using nano-size powders with average grain size of 100 nm by precipitation method. They have investigated the sinterability of the nano-sizepowders, mechanical strength, microstructure and in vitro degradability. Their results revealed that the nano-size powders possess superior sintering characteristics as compared to the micro-size powders. Nano-size β-tricalcium phosphate powders with average grain size of 50 nm were synthesized by wet chemical precipitation method by Mirhadi *et al.* [19] taking calcium nitrate and diammonium hydrogen phosphate as calcium and phosphorus precursors. They concluded that with increasing pH up to 10.8 can increase the Ca/P ratio to 1.59 and alter phase composition of the synthesized powders.

Kohei Nagata *et al.*[20] synthesized β-TCP powders by mechanochemical method. R.Othman *et al.*[21] investigated the different factors affecting the synthesis of beta-tricalcium phosphate powder by a wet precipitation technique. They have concluded that the most optimum factors to synthesize single-phase β-TCP are a stirring speed of 200 rpm for 1 hour, calcination temperature of 900^0C, and a calcination soaking duration of 2 hours.

A. Farzadi *et al.* [22] synthesized and characterized hydroxyapatite/β-tricalcium phosphate nano composites by microwave irradiation. They claimed to have improved crystallinity in comparison with conventional wet chemical method. S. Laasri *et al.*[23] have investigated the effect of powder manufacturing and sintering temperature on densification, microstructure and mechanical characteristics of dense β-tricalcium phosphate (β-TCP) bioceramic. They have showed that the β-TCP can be sintered at 1160°C for 3 hours to have good density and high performance mechanical properties (Vickers hardness, Young's modulus and toughness).

Langlang Liu *et al.*[24] worked on the production, characterization of nano-β-tricalcium phosphate and the inhibition on hepatocellular carcinoma cells. They have investigated the inhibitory effect of nano-β-TCP on HepG2 cells in vitro. They revealed that the average particle size of nano-β-TCP powder was about 72.7 nm and had a certain inhibitory effect on viability of HepG2 cells in a time- and dose-dependent manner. They concluded that nano-β-TCP-based anticancer drug carrier could be treatment modalities in the future.

Ghosh *et al.* [25] synthesized and characterized sintered beta-tricalcium phosphate through three different routes namely, wet chemical co-precipitation, sol-gel and solution combustion synthesis. They compared the effect of preparation route. They have concluded that the pellet developed from

powder manufactured via co-precipitation route achieved maximum density compared to the pellets synthesized from powders via sol-gel and solution combustion method.

F Abida *et al.* [26] characterized tricalcium phosphate powders from calcium hydroxide and ortho-phosphoric acid at room temperature, without pH adjustment and in absence of ionic impurities. The developed powder has an atomic ratio Ca/P of 1.512 ± 0.005. The heat treatment of the powder leads to the condensation of hydrogenophosphate ions to pyrophosphate at 446.60°C, They also showed the transformation of TCPs to β-TCP at 748.56°C and the transformation of β to α TCP at 1167.06 °C.Yunqing Kang *et al.*[27] prepared poly(L-lactic acid)/β-tricalcium phosphate scaffold for bone tissue engineering without organic solvent .They didn't use any organic solvent, which offers an advantage to avoid problems associated with organic solvent residue .

A. Nurazreena *et al.*[28] also synthesized β -tricalcalcium phosphate block by wet milling process by using calcium hydrogen phosphate dihydrate and calcium carbonate. They concluded that the crystallinity and crystallite size of the developed β-TCP increased with increasing pressure and sintering temperature, which was also confirmed by K.P. Sanosh *et al.*[29], who prepared β-tricalcium phosphate nano powders (80 nm) using a simple sol–gel route with calcium nitrate and potassium dihydrogenphosphate as calcium and phosphorus precursors.

High porosity β-TCP and β-TCP/Al_2O_3 scaffolds by Gel-Casting of Foams was developed by Lilian Siqueira *et al.* [30]. They claimed that the developed scaffold showed increased porosity (86-88%) and pore sizes ranging from 200 to 500 μm.

Hyun-Seung Ryu *et al.*[31] made an development in the sintering property of β-tricalcium phosphate by adding calcium pyrophosphate. They investigated the sintering behavior of β-tricalcium phosphate [TCP, $Ca_3(PO_4)_2$] doped with calcium pyrophosphate (CPP, $Ca_2P_2O_7$) . They concluded that pure β-TCP suffers phase transition to α-TCP at about 1200°C; henceforth pure β-TCP ceramics should be sintered below 1200°C. However, the addition of CPP in the range of 0.5–3wt% delays phase shift of β-TCP and enables sintering of β-TCP at 1200°C without a phase transformation to α-TCP. CPP-doped β-TCP ceramics with relative density over 95% could be obtained when sintered at 1200°C for 2 h.

A.Destainville *et al.* [32]synthesized and characterized beta tricalcium phosphate via an aqueous precipitation method. Their results showed high variability of Ca/P ratio of powders with the ripening time, and more particularly an increase of the Ca/P value with the duration. They have reported that the temperature and pH of the reaction medium also play a vital role in the composition of the precipitate.

Bo Li *et al.* [33] synthesized bioactive β-tricalcium phosphate microspheres as bonegraft substitute materials. There are some researchers who have tried to synthesis β-TCP from some biological origin. Akari Takeuchi *et al.*[34] successfully prepared Porous β-tricalcium phosphate (β-TCP) from star fish-derived calcium carbonate (sf-bone) under several hydrothermal conditions.

2.2 Effects of dopants

The chemical alteration of β-TCP by ionic substitution is an attractive topic in the field of advanced biomaterials in recent years. It has been pursued that major components of biological tissues i.e. bone, teeth and some invertebrate skeletons, are composed of calcium phosphate as mineral phase containing a variety of influencing elements [35]. The study of ionic substitutions in β-TCP phase due to effective role of these trace elements (Zn, Mg, Ti, Sr, K, Na etc) in the biological system upon implantation has been well documented from the research reports [36]. The dopants which are widely used include Zn, Mg, Sr. A wide no of publications are there on these dopants and their different kind of subsequent effect on various properties [37-41].Yuqin Qiao *et al.*[42] showed the stimulation of bone growth following zinc incorporation into biomaterials.

Amit Bandyopadhyay *et al.*[43] studied the influence of MgO, ZnO, and SiO_2 dopants on Calcium Phosphate based resorbable ceramics. They incorporated different combinations of dopants into beta tricalcium phosphate ceramic compacts and tested for different characterization. All binary and ternary dopants samples revealed higher densification in comparison with pure β-TCP. They also reported that dopants play a significant role toward improving cell–materials interactions in tissue biology.

Khaled R. Mohamed *et al.* [44] worked on the synthesis and characterization of β-TCP zirconia/polymeric biocomposites for bio-applications. Their results confirmed that zirconia has a major role in the development of apatite formation. P.M.C. Torres *et al.* [45] studied the effect of Mn-doping on the structure, morphology and biological properties of β-tricalcium phosphate. They have reported that higher amount of Mn concentrations lead to decreasing the value of of a- and c-axis lattice parameters, and Mn-doping also significantly changed the morphology of β-TCP powders. Hiroki Nishikawa *et al.* [46] have investigated Zn-Substituted tricalcium phosphate powder by ultrasonic spray-pyrolysis technique. They examined the influence of zinc addition to the crystal structure of TCP and concluded that increasing Zn content did not show a significant change of the a-axis, b –axis and c –axis lattice constants. They also reported that the bulk density of Zn-TCPs showed their maximum value at 1100°C. Rahul Sasidharan Pillai *et al.* [47] investigated the

character of β-TCP powder and its thermal behavior by Mg ion doping. They have suggested from XRD and DTA analyses that 1 mol% MgO-doped samples in the β phase can be stabilized at temperatures as high as 1500°C. V. Graziani *et al*. [48] synthesized Zinc-doped tricalcium phosphate powders as a solid phase of calcium phosphate cement by precipitation from aqueous solutions at 25 °C for functionalized bone grafts applications. They reported that Zn-ion release from CPC-Zn 0.6wt% and CPC-Zn 1.2wt% cements, measured by the Atomic Emission Spectroscopy (AES), corresponded to the average values of 0.3070.01mg/L and 0.1070.01 mg/L, respectively. A.Gozalian *et al*. [49] synthesized Mg-doped calcium phosphate nano powders via the sol gel method and studied their thermal behavior. Their morphological analysis showed that the developed powders were composed of nano particles, with sizes ranging from 40 to 100 nm. In addition they reported that the β-TCP to α-TCP transformation temperature increased due to the influence of magnesium ions. Shashwat S. Banerjee*et al*. [50] investigated the effects of MgO and SrO binary doping on the mechanical and biological properties of β-TCP ceramics. They have reported that MgO and SrO doping improved the β phase stability at a sintering temperature of 1250°C and marginally reduced the compressive strength of β-TCP. Gary Fielding *et al*. [51] suggested that the mixture of SiO_2 and ZnO dopants in TCP may be a major substitute to establish osteoinductive properties to calcium phosphate.

Zinc-containing tricalcium phosphate (Zn-TCP) was synthesized to investigate the role of zinc in osteoblastogenesis, osteoclastogenesis and in vivo bone induction in an ectopic implantation model by XiaomanLuo *et al*. [52.] Their results indicated that zinc incorporated in TCP can modulate bone metabolism and render TCP osteoinductive. The influence of Mg^{2+} doping on beta–alpha phase transition in tricalcium phosphate bioceramics was studied by Matteo Frasnelli *et al*. [53]. They have found that the existence of magnesium within the TCP lattice strongly effects the kinetic of the β ↔ α phase conversion, promoting the spontaneous α →β reconversion even upon fast cooling, or slowing down the β → α transition during heating. Similarly, it allows the α →β transformation in TCP sintered components by optimized annealing treatment at 850 °C.

Sandrine Gomes *et al*. [54] also studied the Cu-doping mechanism in calcium phosphate bio ceramics in the field of biomedical engineering. Susmita Bose *et al*. [55] evaluated the effect of MgO, SrO and SiO_2 doping on mechanical and biological properties of β-tricalcium phosphate taking different combination. They found that compressive strengths for each samples showed degradation in simulated body fluid (SBF) over the 16 weeks time period with varying degradation kinetics. They have reported that MgO/SrO/SiO_2 doped sample showed no loss in strength, for MgO/SrO doped

TCP strength loss is slow and gradual, while undoped TCP shows the maximum strength loss from 419±28 to 158±28 MPa in that period. The effect of ZnO presence and sintering temperature on phase assemblage, microstructure and densification of monophasic/biphasic α /β TCP has been investigated by L. Carbajal *et al.* [56]. They have concluded that the control of the ZnO dopant content and the sintering temperature let the development of different microstructural material configurations attending to β/α TCP phase assemblage and proportions. Satish S. Singh *et al.* [57] synthesized a biphasic mixtures of crystalline β-tricalcium magnesium phosphate (β-TCMP) and an amorphous calcium magnesium phosphate. They have reported that magnesium dopent β-TCP supported the higher smount of hMSC differentiation in comparison to β-TCP, due to the release of increased amounts of bioactive magnesium ions. They have concluded that the release of Ca^{2+} ions from β-TCMP scaffolds also have a role in regulating osteogenic differentiation in bone biology. Meili Zhang et *al.* [58] worked on cobalt substituted β-tricalcium phosphate ceramics. They have suggested that the addition of Co into β-TCP stabilized the β-phase structure and improved the sinterability and is a prospective viable way to increase angiogenic properties through biomaterials.

2.3 In vitro biological performance

The choice of a biomaterial depends on its specific biomedical purpose in order to be useful and long lasting without rejection [59]. The primary requirement for any material as implants inside the body is anti-inflammatory, anti-toxic reactions and anti-allergenic symptoms. It must be biocompatible, bioactive, bioinert, biofunctional and sterilizable [60, 61]. Before implantation inside a living body a developed material must be investigated for its physio-mechanical nature. Many researchers evaluated β-TCP and its different derivatives by different experimental procedures like contact angle determination, haemolysis study, bactericidal effect, MTT Assay, SBF study, degradation study, cell culture, corrosion behavior etc.

Feng-Huei Lin *et al.* [62] worked on the degradation behavior β-TCP by soaking it in distilled water at 37°C for to 30 days. They have reported that in static distilled water, calcium ions may be released from β-TCP into solution during the initial 7 days and then changed into hydroxyapetite (HA) .Susmita Bose *et al.* [55] studied the biological properties of MgO, SrO and SiO_2 doped β-TCP and pure β-TCP. They have reorted that weight gain in SBF was shown by undoped and doped β-TCP samples and both revealed a good apatite growth. They have also reported that improved early stage osteoconduction is better in MgO/SrO doped β-TCP than undoped β-TCP. R. Detsch *et al.* [63] studied on the construction of osteoclast-like cells on HA and β-TCP ceramics. They showed that osteoclast-like cells resulting from a human leukoma monocytic lineage reacts in a different way to

beta-tricalcium phosphate (β-TCP) than to hydroxyapatite (HA) ceramics. They have concluded that for implanting bone substitute materials calcium phosphate ceramics should be taken either for their fast degradation (β-TCP) or for the slow remodeling of the biomaterial (HA). The option of the type of material depends on the place and size of the bone fracture as well as the patient's extracellular matrix stoichiometry in osteoblast cell.

L. Saldana *et al.* [64] studied the effect of Calcium phosphate-based particles on osteogenic maturation of human mesenchymal stem cells (hMSC). They have found that both β-TCP and HA particles were efficiently influenced by hMSC. The in vitro corrosion study and in vivo biodegradation of β-$Ca_3(PO_4)_2$/Mg–Zn composites were analyzed by Kun Yu *et al.* [65]. They found that 10% β-$Ca_3(PO_4)_2$/Mg–6% Zn composites show good corrosion resistance, as observed by a 30 day immersion test and electrochemical measurements in SBF at 37°C. The β-$Ca_3(PO_4)_2$/Mg–6% Zn composite revealed good biocompatibility with the tissue and the vital visceral organs like heart, kidney and liver of rabbits. They have concluded that the corrosion products, such as $Mg(OH)_2$ and $Ca_5(PO_4)_6(OH)_2$, cause better the biocompatibility of the β-$Ca_3(PO_4)_2$/Mg–Zn composite . A. Mina *et al.*[66] studied the biocompatibility behavior of β-tricalcium phosphate –chitosan coatings found on 316L stainless steel. Their cytotoxicity and electro chemical assay suggested that this coating improve cell viability, corrosion resistance and showed better biocompatibility than 316L alone. β-tricalcium phosphate with platelet-rich plasma (PRP) as a potential scaffold for the restoration of bone defects was studied by Chenggong Wang *et al.*[67]. They have evaluated biocompatibility by analyzing the adhesion rate and cytotoxicity of bone marrow stromal cells (BMSCs).They have showed the BMSC adhesion rate on the strengthened β -TCP/PRP composite was >96% after 24 h, with a cell cytotoxicity value of zero. Kyung-Sik Oh *et al.* [68] developed TCP-TiO_2biocomposites and studied their cytocompatibility. They have reported that such composites had potential for bio-medical applications. Nurshuhada MohdNazir*et al.*[69] determined the biocompatibility of β-TCP synthesized by hydrothermal and precipitation method with usual human osteoblast (NHOst) cells. They found no toxicity in case of hydrothermal β-TCP or for precipitation β-TCP.Lilian Siqueira*et al.* [30] have reported that β-TCP and β-TCP/Al_2O_3 scaffolds showed cytocompatibility with no cytotoxic and genotoxic effects.

2.4Animal experimentation study

There are numerous numbers of literatures on the in vivo model animal study by using β- TCP and its dopants to promote bone formation. It has been reported that bone regeneration by biomaterials is

based on materials [70–75]. Many researchers have tried with bone morphogenetic proteins (BMPs) as a growth factor. Howa Begam *et al* [76] suggested that although BMPs increasingly used in various bone related applications but there are still intricacies related to its application. According to her Zn doped HA combined with BMP influenced more osteogenesis as well as antimicrobial property then pure HA. Brihat Chettri *et al*. [77] suggested that addition of zinc dopants alone and in combination with insulin like growth factor-1 would be helpful in further improving the osteoconductivity and osteoinductivity of porous hydroxyapatite scaffold .They have also suggested that zinc doped porous HA implants might give a delivery system for bioactive agents to speed up bone healing and improved anchorage of bone implants in bone related surgery.

Some time many researchers used biphasic calcium phosphate ceramics composed of hydroxyapatite (HA) and beta-tricalcium phosphate (β-TCP). Bone formation was observed in calcium phosphate ceramics, whereas no bone formation was detected in other materials in animal experiments as suggested by Akira Ogose *et al*.[78]. Prominent osteoconductive activity and the biodegradable nature of commercially available beta-tricalcium phosphate (β-TCP,OSferions) have been documented in animal experiments by them .They have observed that prominent bone formation and direct bone connection between preexisting bone and OSferions were evident 28 days after grafting. They have reported that almost the entire TCP exterior was covered by lamellar bone; active osteoblastic lining and attachment of the osteoclast-like giant cells were not seen 72 weeks after implantation.

XiaomanLuo *et al*. [79] studied the bone induction due to Zinc in calcium phosphate in vitro and in vivo model. They have concluded that β-TCP without zinc induced no bone formation. They have further added that the observed bone induction cannot be attributed due to zinc alone, but incorporated zinc in β-TCP can modulate bone metabolism and render β-TCP osteoinductive.

John C Dean *et al*. [80] evaluated the host-bone response to hydroxyapatite/tri calcium phosphate (HAp/TCP)-coated and noncoated titanium fiber metal implants placed in a load-sharing cancellous bone of rabbits. They have concluded that the host reply to titanium fiber metal implants is affected both by HAp/TCP coating and by the site of implantation.

Piattelli*et al*.[81] studied the clinical and histological analysis on biphasic calcium phosphate ceramics (BCP). The BCP composed of 50% hydroxyapatite (HAp) and 50% beta-tricalcium phosphate (β-TCP), was used in man to fill defects, resulting from cyst enucleation. The researchers concluded a good biocompatibility and osteoconductivity of the BCP ceramics.

Naoki Kondo *et al*. [82] in the year 2005 studied on Bone development and resorption of highly purified β-tricalcium phosphate in the rat femoral condyle. They observed that highly purified β-TCP give an early bone conduction, followed by bioresorption of β-TCP and the elimination of large parts of the β-TCP with new bone. Collectively, their results suggested that highly purified β-TCP is a biocompatible, resorbable bioactive ceramic. Samit K. Nandi *et al*. [83] evaluated the porous β -tri-calcium phosphate ceramic as bone replacement in goat model. They have concluded that porous β -tricalcium phosphate based implants enhance bone formation over the extension of the defect. Arjun Dey *et al*. [84] investigated the hydroxyapatite and β-tri calcium phosphate microplasma spray (MIPS) coated pin intra-medullary for bone repair in a rabbit model. They found that in comparison to those of the uncoated pins, the pins coated with both MIPS HAP and β-TCP showed noteworthy increase of alkaline phosphatase up to 15th day of surgery, they further concluded that on a relative scale, the performance of the β- TCP coated intramedullary pins was much superior than that of the pure HAP coated pins and than intramedullary pins which were uncoated.

2.5 Effects of vibration in wound healing/bone remodeling

Fracture and bone related problems are very common. Various methods had been tried for the last few decades to stimulate the bone tissue development. In the year 1969 Levitt *et al*. [85] explained a technique of manufacturing an apatite ceramic from mineral fluorapatiteand recommended the probable application of this apatite ceramic in remedial purposes. Since then calcium phosphate ceramics have been extensively researched for their formulations and clinical uses. Many people have tried with Bone grafts for providing support to cover voids or to improve osseous defects either by autograft or allograft. But they have many noteworthy limitations like donor site injury, insufficient availability in inappropriate form. Immunogenicity and disease transmission are also very common problems associated with allograft.

Over many years peoples have tried to understand the effect of mechanical loading on bone remodeling. The working adaptation procedure of bone was first introduced by German anatomist and surgeon Julius Wolff (1836–1902) in the 19th century. He declared that bone in a healthy person or animal will acclimatize to the loads under which it is placed.If loading on a particular bone rises, the bone will remodel itself over time to become stronger to oppose that sort of loading. He emphasized that the remodeling of cancellous bone structure follow mathematical rules analogous to the stress trajectories [86-87].

Osteocytes, cells embedded within our bones, stimulate bone development in the presence of mechanical stimulus, as well as bone degradation in the absence of such stimuli.Thus, mechanical loads that form tiny strains within the bone matrix are somehow felt by the cells inside bone, which then take action to conserve bone mass [88]. For this reason mechanical loads have been applied in many ways by many researchers to study faster bone healing.

John p. Jankovlch [89] studied the influence of mechanical loading on bone regeneration in the rat. He concluded that chronic vibration tries to amplify firmness and microhardness of bone modulus of elasticity and microhardness of vibrated bone than those of non-vibrated bone. Yasuo Usui *et al*. [90] suggested that the mechanical vibration had a favorable effect on callus volume, possibly due to the prompt stimulation of secondary bone healing processes.

Duncan *et al*. [91] suggested that dynamic loading, which is related with extracellular fluid flow and the formation of streaming potentials within bone, is most efficient for stimulating new bone development in vivo. Mechanical loading can slow down bone resorption and boost new bone development in vivo. The results of mechanical loading are related with the magnitude, duration, and rate of the applied load. Longer period, lower amplitude loading has the similar effect on bone formation as of loads with short period and high amplitude.

Flieger J *et al*. [92] evaluated the effects of vibration on bone mineral density and bone mechanical characteristics in a model of ovariectomized rats. They suggested that vibration is a stimulation which prevents postmenopausal bone loss in ovariectomized rats. Narcís Gusi *et al*. [93] worked on Low-frequency vibratory exercise and concluded that this kind of exercises decreases the danger of bone breakage more than walking.They projected that a vibration load with small amplitude (3 mm) and averageintensity, could be used to stop age-related bone loss at the hip, especially in fragile populations.

Wenger K H *et al*. [94] investigated with two different level of vibration at same frequency. They revealed that there was a constant move toward higher mean density in the bone density spectrum (BDS), with the two vibration levels. Klein-Nulend J *et al*. [95] concluded that osteocyte cytoskeleton, which ultimately modulates cell shape, is a primefactor in determining how osteocytes sense stresses, whether by a local or bulk deformation, or via a relocation of forces inside of the cell. As osteocytes redesign bone remodelling, any aspect affecting the osteocyte cytoskeleton and thereby the osteocyte response to mechanical stimuli, certainly affects bone mass ratio.

In bone biology, load is powerful determinants, affecting bone tissue development, mass, morphology, repair, and aging as described by Ozcivici *et al.* [96].

Zhang C *et al.* [97] demonstrated that small magnitudeand high frequency mechanical vibration encourages osteogenic differentiation of periodontal ligament stem cells (PDLSC) and implies the presence of a frequency-dependent effect of vibration on determining PDLSC commitment to the osteoblast lineage. Kulkarni R N *et al.* [98] suggested that mechanical vibration of osteoclast precursor cells down streams the DC-STAMP expression in osteoclast ancestor cells leading to the reduction of osteoclast development. Mechanical vibration could be a non-pharmaceutical management for treatment of osteoporosis .Weinheimer-Haus Eileen M. *et al.* [99] investigated a therapeutic move toward the wound healing by applying whole body low-intensity vibration (vibration with a magnitude less than 1g acceleration). They concluded that low-intensity vibration (LIV) may produce beneficial effects on wound healing by improving angiogenesis and granulation tissue development, and these changes are related with increases in pro-angiogenic growth factors. Zhou,Yi *et al.* [100] explained the beneficial role of WBV in increasingosteointegration in the osteoporotic status. Osteoblasts seem to be the main target cells in the vibration-induced anabolic but anti-resorptive effect in bone. At the transcript and protein levels, WBV drives genes and proteins, which play an important role in vibration-induced bone remodeling.

Melis *et al.* [101] came to conclusion through a thorough review that low intensity vibration (LIV) signals are secure and anticatabolic for skeletal system cells and are of great importance in regenerative medicine. Studies so far indicated that there are obvious effects on bone during different condition of vibration. There are many doubts related with the application of whole body vibration.

Ete Chan M *et al.* [102] clearly mentioned that before Whole Body Vibration (WBV) can be taken as a means of eliminating the threat of fractures due to osteoporosis, the risks of acute and or chronic exposure to vibration must be analyzed relative to the potential benefits of treatment. Regardless of the growing number of studies which point out that vibration applied over a range of durations, frequencies and intensities can be anabolic and anti-catabolic to musculoskeletal system, concern must also be emphasized as vibration is a known pathogen to many physiologic systems and at higher intensities may cause the fracture more worsen than betterment [103]. Thus, a whole body vibration procedure is an uncontrolled strategy and can lead to deposit unwanted minerals that can unnecessarily stiffen other bones.

References

[1] F.H.Albee,AnnSurg ,71(1920) 32

[2] E. B. Nery,K.L.Lynch and W.M.Hirthe,J Periodontol,63 (1975) 729

[3] H.W. Denissen,PhDThesis,Amsterdam,Vrije Universiteit (1979)

[4] M Jarcho ,Clin, orthop,157(1981) 259

[5] K Degroot, "Bioceramics of Calcium Phosphate" (CRC press, Boca Raton 1983)

[6] S D Metsger,T.D.Driskell and J R Paulsrud, J Am Dent, Assoc.105(1982)1035

[7] Pramanik, S., Agawal, A. K., Rai, K. N. & Garg, A. 2007. Development of high strength hydroxyapatite by solid-state-sintering process. Ceramic International. 33: 419-426.

[8]H.S. Liu, T.S. Chin, L.S.Lai, S.Y.Chiu, K.H.Chung, C.S.Chang, M.T.LuiHydroxyapatite synthesized by a simplified hydrothermal method,CeramicsInternationalVolume 23, Issue 1, Pages 19-25,1997

[9] Kwon S, Jun Y, Hong S and Kim H, Synthesis and dissolution behavior of β-TCP and HA/β-TCP composite powders J. Eur.Ceram. Soc. 23 1039–45 23 909–14, 2003

[10] Yeong, K. C. B., Wang, J. & Ng, S. C. Mechanochemical synthesis of nanocrystalline hydroxyapatite from CaO and CaHPO4. Biomaterials.22:2705-2712.2001

[11] Kumar, T. S. S., Manjubala, I. & Gunasekaran, J. Synthesis of carbonated calcium phosphate ceramic using microwave irradiation,Biomaterials. 21: 1623-1629. 2000

[12]Xinlong Wang ,Hongsong Fan , Yumei Xiao , Xingdong Zhang, Fabrication and characterization of porous hydroxyapatite/β-tricalciumphosphate ceramics by microwave sintering, Materials Letters 60, 455–458, 2006.

[13] Tas, A.C., Combustion synthesis of calcium phosphate bioceramic powders.Journal of the European Ceramic Society. 20: 2389-2394. 2000.

[14].Bow J, Liou S and Chen S, Structural characterization of room-temperature synthesized nano-sized β-tricalcium phosphate Biomaterials 25 3155–61,2004.

[15]. Gunduz, Oguzhan. A Simple Method of Producing Hydroxyapatite and Tri Calcium Phosphate from Coral (Pocilloporaverrucosa).Journal of the Australian Ceramic Society. 50. 52-58, 2014.

[16]. Siddharthan A, Seshadri S K and Sampath Kumar T S, Rapid synthesis of calcium deficient hydroxyapatite nanoparticles bymicrowave irradiation trends Biomater. Artif. Organs 18 110–3,2005

[17]. M. Jarcho et al Journal of Materials Science 14 142-1S0,1979.

[18]. K. Lin, J. Chang, J. Lu, W. Wu, Y. Zeng, "Properties of β-$Ca_3(PO_4)_2$bioceramics prepared using nano-size powders", Ceram. Int., 33 979–985,2007.

[19].Bahman Mirhadi, Behzad Mehdikhani, NayerehAskari, Synthesis of nano-sized β-tricalcium phosphate via wet precipitation, Processing and Application of Ceramics 5 [4] 193–198,2011.

[20].Kohei Nagata, ToshiisaKonishi, Michiyo Honda, Mamoru Aizawa, Preparation and Characterization of β-Tricalcium Phosphate Powders with High Solubility for Chelate-Setting Calcium-Phosphate Cements, Key Engineering Materials, Vol. 758, pp 194-198, 2017.

[21].R.Othman, Z.Mustafa, P.T. Kien, N.F. Ishak, A. Shaaban and A.F. MohdNoor,Parameters affecting the synthesis of Beta-tricalcium phosphate powder using a wet precipitation method ,Journal of Mechanical Engineering and Sciences,Volume 11,Issue 4, pp.3197-3205, December 2017.

[22].A. Farzadi , M. Solati-Hashjin, F. Bakhshi, A. Aminian, Synthesis and characterization of hydroxyapatite/b-tricalcium phosphate nanocomposites using microwave irradiation Ceramics International 37 65–71,2011.

[23].S. Laasri , M. Taha, E.K. Hlil , A. Laghzizil , A. Hajjaji ,C. R. Mecanique 340, 715–720,2012.

[24].Langlang Liu, Yanzeng Wu, Chao Xu, Suchun Yu, Xiaopei Wu, and Honglian Dai, Synthesis, Characterization of Nano-β-Tricalcium Phosphate and the Inhibition on Hepatocellular Carcinoma Cells , Journal of Nanomaterials, Article ID 7083416, pg 1-7, 2018

[25]. R Ghosh , R Sarkar, Synthesis and characterization of sintered beta-tricalcium phosphate: A comparative study on the effect of preparation route Materials Science and Engineering ,C 67 345–352,2016.

[26].Fatima Abida, MostafaElassfouri, Mohamed Ilou, Bahiya El ouatli, Mohamed Jamil, NawalMoncif and ZinebHatim ,Tricalcium phosphate powder: Preparation, characterization and compaction abilities ,Mediterranean Journal of Chemistry, 6 (3), 71-76, 2017.

[27]. Yunqing Kang, GuangfuYin ,Quan Yuan , Yadong Yao , Zhongbing Huang , Xiaoming Liao , Bo Yang , Li Liao , Hui Wang, Preparation of poly(L-lactic acid)/β-tricalcium phosphate scaffold for bone tissue engineering without organic solvent, Materials Letters, 62, 2029–2032, 2008.

[28]. Nurazreena and K.S. Lau, Synthesis of β -tricalcalcium phosphate Block by Wet Milling Method of Calcium Hydrogen Phosphate Dihydrate and Calcium Carbonate, Advanced Materials Research Vol. 1087 , 384-388, 2015.

[29].K.P. Sanosh , Min-Cheol Chu , A. Balakrishnan , T.N. Kim , Seong-Jai Cho ,

Sol–gel synthesis of pure nano sized β-tricalcium phosphate crystalline powders, Current Applied Physics 10 68–71, 2010.

[30] LilianSiqueira, Cynthia Guimarães de Paula, Mariana Motisuke, RubiaFigueredoGouveia, Samira EstevesAfonso Camargo, NoalaVicensoto Moreira Milhan, Eliandra de Sousa Trichês, Preparation, Characterization and Biological Studies of β-TCP and β-TCP/Al_2O_3 Scaffolds Obtained by Gel-Casting of Foams, Materials Research, 20(4): 973-983, 2017.

[31]Hyun-SeungRyu, Hyuk-JoonYoun, Kug Sun Hong, Bong-Sun Chang, Choon-Ki Lee, Sung-Soo Chung, An improvement in sintering property of β-tricalcium phosphate by addition of calcium pyrophosphate, Biomaterials 23, 909–914, 2002.

[32]A. Destainville, A. Rolo, E. Championand D. BernacheAssollant, Synthesis and Characterization of beta tricalciumPhosphate ,Key Engineering Materials ,Vols. 240-242, pp 489-492,2003.

[33] Bo Li , Zhongning Liu, Jingwen Yang, Zhongchao Yi , Wenqian Xiao , Xue Liu , Xiaoling Yang ,WenfengXu, Xiaoling Liao , Preparation of bioactive β-tricalcium phosphate microspheres as bonegraft substitute materials , Materials Science and Engineering C 70, 1200–1205,2017.

[34]Akari Takeuchi, TomohitoTsuge , Masanori Kikuchi , Preparation of porous β-tricalcium phosphate using starfish-derived calcium carbonate as a precursor, Ceramics International 4215376–15382,2016.

[35]. S. Kannan, F.Goetz-Neunhoeffer, J.Neubauer ,S. Pina ,P.M.C. Torres ,J.M.F.Ferreira, Synthesis and structural characterization of strontium and magnesium-co-substituted b-tricalciumphosphate,ActaBiomaterialia 6, 571–576, 2010.

[36] Howa Begam , Somali Mandal , Abhijit Chanda , Jayanta Mukherjee and Samit Kumar Nandi Effect of Zinc Doping on Biological Properties of Biphasic Calcium Phosphate Ceramics in Orthopaedic Animal Model Trans. Ind. Ceram. Soc., vol. 73, no. 4, pp. 284-292,2014.

[37]. Promita Bhattacharjee, Howa Begam, Abhijit Chanda, Samit Kumar Nandi, Animal trial on zinc doped hydroxyapatite: A case study ,Journal of Asian ceramic Societies,(2)44-51, 2014

[38]. Bigi A, Foresti E, Gandolfi M, Gazzano M, Roveri N. Isomorphous substitutions in β-TCP: the different effects of zinc and strontium, J Inorg Biochem;66:259–65, 1997.

[39]. Kannan S, Pina S, Ferreira JMF. Formation of strontium-stabilized b-tricalcium phosphate from calcium-deficient apatite. J Am Ceram Soc; 89:3277–80, 2006.

[40].Enderle R, Göetz-Neunhoeffer F, Göbbels M, Müller FA, Greil P. Influence of magnesium doping on the phase transformation temperature of β-TCP ceramics examined by Rietveld refinement,Biomaterials;26:3379–842005.

[41].Kannan S, Ferreira JMF. Synthesis and thermal stability of hydroxyapatite-b tricalcium phosphate composites with co substituted sodium, magnesium, and fluorine, Chem Mater,18:198–203,2006.

[42] YuqinQiao , Wenjie Zhang , PengTian , FanhaoMeng , Hongqin Zhu ,Xinquan Jiang , Xuanyong Liu , Paul K. Chu Stimulation of bone growth following zinc incorporation into Biomaterials, Biomaterials 35 6882-6897,2014.

[43] Amit Bandyopadhyay, W Sheldon Bernard, WeichangXue, and Susmita Bose Calcium Phosphate-Based Resorbable Ceramics: Influence of MgO, ZnO, and SiO_2 Dopants J. Am. Ceram. Soc., 89 [9] 2675–2688,2006.

[44] Khaled R. Mohamed a, Amr M. Mohamed b, Hanan H. Beherei, Synthesis and in vitro behavior of b-TCP zirconia/polymeric biocomposites for bio-applications ,Journal of Genetic Engineering and Biotechnology 9, 111–119,2011.

[45]P.M.C. Torres , S.I. Vieira , A.R. Cerqueira , S. Pina , O.A.B. da Cruz Silva ,J.C.C. Abrantes , J.M.F. Ferreira Effects of Mn-doping on the structure and biological properties of β-tricalcium phosphate, Journal of Inorganic Biochemistry 136 57–66, 2014.

[46]Hiroki Nishikawa, Michiyo Honda, Tomohiro Yokota, Yusuke Shimizu, and Mamoru Aizawa,Preparation of Spherical Zn-Substituted Tricalcium Phosphate Powder by Ultrasonic Spray-Pyrolysis Technique and Its Characterization, Journal of Nanomaterials Volume 2016, Article ID 6753203, 2016.

[47] Rahul SasidharanPillai, Vincenzo M.Sglavo, Effect of MgO addition on solid state synthesis and thermal behavior of beta-tri calcium phosphate, Ceramics International 412512–2518, 2015.

[48]V. Graziani, M.Fosca, A.A.Egorov , Yu.V.Zobkov , A.Yu.Fedotov , A.E.Baranchikov , M. Ortenzi , R.Caminiti , V.S.Komlev , J.V.Rau, Zinc-releasing calcium phosphate cements for bone substitute materials, Ceramics International,4217310–17316,2016.

[49]A. Gozalian , A. Behnamghader, M. Daliri , A. Moshkforoush, Synthesis and thermal behavior of Mg-doped calcium phosphate nanopowders via the sol gel method , Scientia Iranica F 18 (6), 1614–1622,2011.

[50] Shashwat S. Banerjee , SolaimanTarafder , Neal M. Davies , AmitBandyopadhyay , Susmita Bose, Understanding the influence of MgO and SrO binary doping on the mechanical and biological properties of b-TCP ceramics, ActaBiomaterialia ,6 4167–4174, 2010.

[51] Gary Fielding, Susmita Bose, SiO_2 and ZnO dopants in three-dimensionally printed tricalcium phosphate bone tissue engineering scaffolds enhance osteogenesis and angiogenesis in vivo, ActaBiomaterialia 9 913 7–9148, 2013.

[52]XiaomanLuo , DavideBarbieri , Noel Davison , Yonggang Yan , Joost D. de Bruijn , Huipin Yuan Zinc in calcium phosphate mediates bone induction: In vitro and in vivo Model, ActaBiomaterialia 10, 477–485,2014.

[53] MatteoFrasnelli, Vincenzo M. Sglavo, Effect of Mg2+ doping on beta–alpha phase transition in tricalcium phosphate (TCP) bioceramics , ActaBiomaterialia 33, 283–289, 2016.

[54]Sandrine Gomes, Charlotte Vichery , StéphaneDescamps , Hervé Martinez , AmandeepKaur , Aurélie Jacobs , Jean-Marie Nedelec , Guillaume Renaudin, Cu-doping of calcium phosphate bioceramics: From mechanism to the control of cytotoxicity , ActaBiomaterialia 65 ,462–474,2018.

[55]Susmita Bose , SolaimanTarafder, Shashwat S. Banerjee , Neal M. Davies , AmitBandyopadhyay Understanding in vivo response and mechanical property variation in MgO, SrO and SiO_2 doped β-TCP, Bone 48 1282–1290 , 2011.

[56] L. Carbajal, A. Caballero, M.A. Sainz, Design and processing of ZnO doped tricalcium phosphate based materials: Influence of β/α polymorph phase assemblage on microstructural evolution, Journal of the European Ceramic Society, 32 569–577, 2012.

[57]Satish S. Singh , Abhijit Roy , Boeun Lee , Ipsita Banerjee , Prashant N. Kumta, Synthesis, characterization, and in-vitro cytocompatibility of amorphous β-tri-calcium magnesium phosphate ceramics, Materials Science and Engineering, C 67 636–645,2016.

[58]Meili Zhang, Chengtie Wu, Haiyan Li, Jones Yuen, Jiang Chang and Yin Xiao Preparation, characterization and in vitro angiogenic capacity of cobalt substituted β-tricalcium phosphate ceramics, J. Mater. Chem., , 22, 21686,2012.

[59]. Chen, Q., Thouas, G.A.: Metallic implant biomaterials. Mat. Sci. Eng. R. 87, 1–57 (2015)

[60]. Bauer, S., Schmuki, P., Von Der Mark, K., Park, J.: Engineering biocompatible implant surfaces Part I: materials and surfaces. Prog. Mater Sci. 58, 261–326 ,2013.

[61]. Domanska, A., Boczkowska, A: Biodegradable polyurethanes from crystalline prepolymers. Polym.Degrad. Stab. 108, 175–181,2014.

[62] Feng-Huei Lin, Chun-Jen Liao, Kao Shao Chen, Jui-Sheng Sun and Haw-Chang Liu,Degradation behaviour of a new bioceramic: $Ca_2P_20_7$ with addition of of $Na_4P_20_7.10H_20$, Biomaterials 18, 915-921,1997.

[63] R. Detsch, H. Mayr, G. Ziegler, Formation of osteoclast-like cells on HA and TCP ceramics, ActaBiomaterialia 4 139–148, 2008.

[64] L.Saldana, S. Sa´nchez-Salcedo , I. Izquierdo-Barba, F. Bensiamar , L. Munuera , M. Vallet-Regı´, N. Vilaboa,Calcium phosphate-based particles influence osteogenic maturation of human mesenchymal stem cells,ActaBiomaterialia 5 1294–1305,2009.

[65] Kun Yu, Liangjian Chen, Jun Zhao a, ShaojunLi ,Yilong Dai , Qiao Huang , Zhiming Yu ActaBiomaterialia 8 2845–2855,2012.

[66]A. Mina , H.H. Caicedo , J.A. Uquillas , W. Aperador , O. Guti_errez, J.C. Caicedo Biocompatibility behavior of β-tricalcium phosphate-chitosancoatings obtained on 316L stainless steel, Materials Chemistry and Physics 175, 68-80,2016.

[67] Chenggong Wang, Da Zhong, Xing Zhou, Ke Yin, Qiande Liao, Lingyu Kong And Ansong Liu, Preparation of a new composite combining strengthened β-tricalcium phosphate with platelet-rich plasma as a potential scaffold for the repair of bone defects, Experimental And Therapeutic Medicine 8: 1081-1086, 2014.

[68] Kyung-Sik Oh, Florence Caroff, Roger Famery, Marie-Francoise Sigot-Luizard and Philippe Boch Preparation of TCP-TiO_2Biocomposites and Study of Their Cytocompatibility, J.European cerami soc,18,1931-37,1998.

[69]NurshuhadaMohdNazir, DasmawatiMohamad,Md. AzmanSeeni Mohamed, Nor Shamsuria Omar, Radzali Othman, Biocompatibility of in house β-tricalcium Phosphate ceramics with normal Human osteoblast cell, Journal of Engineering Science and Tech,Vol. 7, No. 2 169 - 176 ,2012

[70]Calcium Phosphate Bioceramics: A Review of Their History, Structure, Properties, Coating Technologies and Biomedical Applications.NoamEliaz and Noah Metoki Materials 2017, 10, 334

[71] F.H. Albee, Studies in bone growth, Ann. Surg. 71 32–39,1920.

[72] H.U. Cameron, I. Macnab, R.M. Pilliar, Evaluation of a biodegradable ceramic, J. Biomed.Mater. Res. 11, 179–186. 1977.

[73] E.B. Nery, K.L. Lynch, G.E. Rooney, Alveolar ridge augmentation with tricalcium phosphate ceramic, J. Prosthet. Dent. 40 668–675,1978.

[74] D.M. Roy, S.K. Linnehan, Hydroxyapatite formed from coral skeletal carbonate by hydrothermal exchange, Nature 247 220–222,1974.

[75] W. Brown, L. Chow, A new calcium-phosphate setting cement, J. Dent. Res. 62 , 672. 1983

[76] Howa Begam,S K Nndi, B Kundu,AChanda,Strategies for delivering bone morphogenetic protein for bone healing ,Materials Science and Engineering C 70 856-869, 2017.

[77] BrihatChettri ,Samit Kumar Nandi , Abhijit Chanda and Howa Begam, Bone Ingrowth to Insulin like Growth Factor-1 Loaded Zinc Doped Hydroxyapatite Implants: an In Vivo Study , Open Access Scientific Reports, Volume 1 , Issue 4 , (2-9), 2012.

[78]Akira Ogose, Naoki Kondo, Hajime Umezu, Tetsuo Hotta,Hiroyuki Kawashima, Kunihiko Tokunaga, Tomoyuki Ito, Naoko Kudo,Makiko Hoshino, Wenguang Gu, Naoto Endo ,Histological assessment in grafts of highly purified beta-tricalciumphosphate (OSferions) in human bones, Biomaterials 27, 1542–1549,2006.

[79]XiaomanLuo ,DavideBarbieri , Noel Davison, Yonggang Yan, Joost D. de Bruijn, Huipin Yuan Zinc in calcium phosphate mediates bone induction: In vitro and in vivo Model , ActaBiomaterialia 10, 477–485,2014.

[80] John C. Dean, MD, Chris L. Tisdel, MD, Victor M. Goldberg, MD, Jack Parr, PhD, Dwight Davy, PhD and Sharon Stevenson, DVM, PhD, Effects of Hydroxyapatite Tricalcium Phosphate Coating and Intracancellous Placement on Bone Ingrowth in Titanium Fibermetal Implants, The journal of Arthoplasty Vol. 10 No. 6 1995.

[81]A. Piattelli, A. Scarano and C. Manganot, Clinical and histologic aspects of biphasic calcium phosphate ceramic (BCP) used in connection with implant placement, 0142-9612 (95) 00342-8.

[82] N. kondu,AOgoseet al Osteoinduction with highly purified β-tri calcium phosphate in dog dorsal muscles and the proliferation of osteoclasts before hetero topic bone formation,Biomaterials 27,4419-4427,2006.

[83].S K Nandi,S K Ghosh,BKundu, D K De,D,Basu,Evaluation of porus β-tri calcium phosphate ceramic as bone substitute in goat model,Small Ruminant research.75,144-153,2008

[84]ArjunDey , Samit Kumar Nandi , BiswanathKundu ,Chandrasekhar Kumar , Prasenjit Mukherjee , Subhasis Roy ,Anoop Kumar Mukhopadhyay , Mithlesh Kumar Sinha, DebabrataBasu,Evaluation of hydroxyapatite and b-tri calcium phosphate microplasmaspray coated pin intra-medullary for bone repair in a rabbit model, Ceramics International 37, 1377–1391,2011.

[85]. Levitt, G. E., Crayton, P. H., Monroe, E. A. &Condrate, R. A., Forming methods for apatite prosthesis. J. Biomed. Mater. Res., 3 ,683-685.1969

[86]J.B Park, Biomaterials Science and Engineering ,Plenum Press, NY & London

[87]Wolff's law and bone's structural adaptations to mechanical usage: an overview for the clinicians" Harold M. Frost, The angle orthodontist, Vol. 64(3).175-188.1994

[88] Klein-Nulend J, Bacabac R.G. and Bakker A.D. Mechanical Loading And How It Affects Bone Cells: The Role Of The Osteocyte Cytoskeleton In Maintaining Our Skeleton. European Cells and Materials Vol. 24 , 278-291 ,2012.

[89] Jankovlch John P, The Effects Of Mechanical Vibration On Bone Development In The Rat.J Biomechanics, Vol.5, 241-250,1972.

[90] Usui Y,.Zerwekh Joseph E, Vanharanta H, "Richard B. Ashman, Vert Mooney, Different Effects of Mechanical Vibration on Bone In growth into Porous Hydroxyapatite and Fracture Healing in a Rabbit Model, Journal of Orthopaedic Research, vol. 7, 559-567, 1989.

[91] Duncan L R, ,Turner H C,Mechanotransduction and the functional response of bone to mechanical starain , Calcif Tissue Int 57:344-358,1997.

[92]. J. Flieger,.KarachaliosTh,.Khaldi L,.Raptou P,.Lyritis G, Mechanical Stimulation in the Form of Vibration Prevents Postmenopausal Bone Loss in Ovariectomized Rats Calcif Tissue Int, 63:510–514,1998.

[93] Narcís Gusi, Armando Raimundo, Alejo Leal, Low-frequency vibratory exercise reduces the risk of bone fracture more than walking: a randomized controlled trial, BMC Musculoskeletal Disorders, 7:92, 2006.

[94]. Karl H. Wenger et al., Effect of whole-body vibration on bone properties in aging mice , Bone 47, 746–755,2010.

[95] KleinNulend, J.; Bacabac, R.G.; Bakker, A.D Mechanical loading and how it affects bone cells: the role of the osteocyte cytoskeleton in maintaining our skeleton . European Cells & Materials, 24, 278-291,2012.

[96].Ozcivici E, Luu YK, Adler B, et al. Mechanical signals as anabolic agents in bone. Nat Rev Rheumatol; 6:50–59, 2010.

[97] Zhang C, Li J, Zhang L, Zhou Y, Hou W, Quan H, Li X, Chen Y, Yu H.Effects of mechanical vibration on proliferation and osteogenic differentiation of human periodontal ligament stem cells. Archives of Oral Biology 57, 10, 1395-1407.2012

[98]KulkarniRishikesh N, A Philip. Voglewede , Liu Dawei, Mechanical vibration inhibits osteoclast formation by reducing DC-STAMP receptor expression in osteoclast precursor cells , Bone 57, 493–498,2013.

[99] Weinheimer-Haus Eileen M, Judex Stefan, Ennis William J.,.Koh Timothy J.Low-Intensity Vibration Improves Angiogenesis and Wound Healing in Diabetic Mice . PLOS ONE,9(3,) e 91355

[100] Zhou Y, Guan X, Liu T, Wang X, Yu M, Yang G, Wang H ,Whole body vibration improves osseointegration by up-regulating osteoblastic activity but down-regulating osteoblast-mediated osteoclastogenesis via ERK1/2 pathway ,Bone 71, 17–24,2015.

[101].Melis OLÇUM, Öznur BASKAN, Özge KARADAŞ, EnginÖZÇİVİCİ,Application of low intensity mechanical vibrations for bone tissue maintenance and regeneration,Turk J Biology, 40: 300-307, 2016.

[102] Chan Ete M &Uzer G &. Rubin C. T,The Potential Benefits and Inherent Risks of Vibration as a Non-Drug Therapy for the Prevention and Treatment of Osteoporosis,Curr Osteoporos Rep ,11:36–44,2013.

[103] M. Ete Chan &GunesUzer& Clinton T. Rubin,The Potential Benefits and Inherent Risks of Vibration as a Non-Drug Therapy for the Prevention and Treatment of Osteoporosis CurrOsteoporos Rep 11:36–44, 2013.

CHAPTER: 3

SCOPE OF THE WORK

& OBJECTIVE

Scope of the work

Numbers of studies have been done so far on the biological performance of TCP and its further improvement. Some workers tried to make it more osteoconductive by adding some dopants, or by making it more porous or by making a combination of HAP and TCP complex. Many attempts have been made to improve the healing process by simple application of these bone substitutes. To achieve the faster healing with some additional effects, site specific application of dynamic loading has also been tried but the results are not yet well explained.

Only a few animal trial reports on TCP are available till date. Study on zinc, magnesium and titanium based beta TCP were not done extensively in animal model so far although these ions are reported to play a significant role in improving cell–materials interactions. Most of the previous works addressed the effect of doping on the enhancement of mechanical, physical properties and on in vitro cell culture experiment.

There are a number of literatures based on the application of whole body vibration for wound healing. Despite the growing number of studies which indicate that vibration delivered over a range of durations, frequencies and intensities can be anabolic and anti-catabolic to musculoskeletal system, caution must also be emphasized as vibration is a known pathogen to many physiologic systems and at higher intensities may cause the very fracture it is intended to prevent. Thus, a whole body vibration procedure can lead to deposition of unwanted minerals, increased stiffness of other bone.

In this context it may be noted that there is no work where the loading is given on a particular damaged area where healing is needed. We did not find any literature where established bone substitutes were applied in the healing zone simultaneously with loading, which, we envisage, can be very much effective for faster healing.

Therefore the identified scopes of the work are mentioned below:

1. Application of loading on a particular damaged area where healing is needed

2. Application of established bone substitutes in the healing zone simultaneously with loading which can be very much effective for faster healing, is to be done

3. A thorough systematic animal study on TCP and its different dopants in loading and unloading condition is to be carried out.

Objective:

The objectives of the proposed works are:

1. To develop pure and doped varieties of β-TCP and to conduct their physical, mechanical and in-vitro biological studies.
2. To conduct dedicated experiment/animal trial to understand the effect of site specific dynamic loading (in the form of axial oscillatory vibration) on new bone formation with and without β-TCP based implant.
3. To compare the biological performance of all varieties of β-TCP with dynamic loading and to select the best one.

CHAPTER: 4

MATERIALS & METHODS

In this chapter, details of the sample preparation, descriptions of materials and methods as well as characterization of the ceramic composites have been discussed.

Physical Characterization:

4.1.1 Preparation of β- Tricalcium phosphate:

β-TCP powder was prepared by a wet chemical precipitation process using the reactants A.R. grade Calcium Carbonate [$CaCO_3$] and orthophosphoric acid [H_3PO_4] both were procured from MERCK, INDIA Ltd., India.

0.6M orthophosphoric acid was taken in a stoichiometric amount in a flask with stop cock. In a beaker distilled water was taken and was heated at 80^0C.This was done on a hot plate with magnetic stirrer. The Calcium Carbonate was added to the warm water (by taking a small amount each time) with the help of a spatula for about 30 mints. Once all the Calcium Carbonate was added to the water, the orthophosphoric acid was added by opening the stop cock very slowly. The whole amount was added to the Calcium Carbonate by taking 30mints minimum addition time. The magnetic stirrer helps in homogeneous mixing and facilitates the reaction. During the reaction the pH was maintained from 11-12 at 80°C. The solution thus obtained was aged for 24 hr followed by filtration. The precipitate was allowed to dry at 80°C for 24 hr, then subsequently calcined at 800°C for 2 hr to obtain the optimum crystallinity. The calcined powder was ball milled to get fine particles.

4.1.2 Preparation of doped β- TCP:

In order to synthesize doped β-TCP powder (Zinc , Magnesium,Titanium doping) measured quantities of zinc oxide (ZnO, 99% pure) , magnesium chloride ($MgCl_2$, $6H_2O$, 98% pure) and and Titanium oxide (TiO_2,99% pure) were incorporated into the Calcium carbonate before its addition to H_3PO_4 solution. In this study, 3 wt% and 5 wt% substitution were made. The developed product was kept aside for 24 hours. After this aging the product was filtered through Buckner funnel and the yield material was taken in petri dish and kept in a hot air oven for 24 hours. The resultant dry product was then calcined at 800ºC for 2 hrs in a electrically heated furnace at a constant heating rate of 5ºC/min.The furnace was then kept to cool for 24 hrs.

4.1.3 Powder Compaction and Sintering Study

The synthesized pure and doped crystalline β-TCP powders were uniaxially hard-pressed using a steel mold having an internal diameter of 10 mm at a pressure of 150MPa, with a 2-ton press for 2 min from PEECO hydraulic pressing machine (PEECO Pvt Ltd, M/C NO.-3/PR-2/HP-1/07-08). Green ceramic structures were measured for their density.

4.1.4 Sintering of dense ceramics:

Almost all ceramic bodies must be sintered to produce a microstructure with the required properties. The green pellets were sintered in a chamber furnaceat 1000ºC and 1100 ºC for 2 hrs at a constant heating rate of 5ºC/min.Some of the sintered samples were crushed into powders, using an agate mortar & a pestle and subsequently sieved to maintain a uniform particle size.The powders thus obtained were first studied for the phase-composition, crystallinity, etc. by X-ray diffraction (XRD) method. Fourier Transformed Infrared Spectroscopy (FTIR) was also performed to further establish the phases formed due to incorporation of zinc as dopant. Further, the dense samples were examined under Scanning Electron Microscope to study their surface morphology and the microstructure.

4.1.5 Green and Sintered Density:

The green and sintered density (gm/cm^3) of the ceramic specimens were measured from mass (M) to volume (V), determined by dimensional measurement) ratio of the specimens. The weights were measured by a weight machine (Sartorius, Model No-BT 2245) and diameter (mm), radius (mm) and thickness (mm) of all green and sintered samples were measured by digital Vernier caliper.

Density = M/V ,Volume = $\pi r^2 h$

4.1.6 Percentage of diametric, linear and volumetric shrinkage:

The dimension of all the green and sintered pellets were measured with the digital Vernier scale .These values were taken for the calculation of Percentage of diametric, linear and volumetric shrinkage. For example, if X_1 could be the initial diameter and X_2 is the sintered diameter of a pellet then the percentage of diametric shrinkage could be $\{(X_1 - X_2)/ X_1\}100$.

4.1.7 Average grain size and pore size:

The pore size, grain size are measured by perfect screen ruler software .We have analyzed five random SEM pictures of each sample, all of same magnification.

4.1.8 Apparent Porosity Measurement: This measurement is done by following the liquid immersion technique [1, 2].The developed pellets has been thoroughly dried and then it is placed in a vacuum chamber for 30 minutes. Without releasing the vacuum, water is then introduced into the chamber and allowed to cover the pellets. Then the chamber is pressurized for a period of 1 hour to ensure the saturation as described by ASTM [1] .The percentage porosity can then be calculated as follows:

Apparent porosity $\phi = \frac{Ww - Wd}{Ww - Ws} \times 100$

Where the terms,

W_d= weight of the dry sample.

Ws= weight of sample immerged in water.

W_W= weight of the saturated sample after removed from the water.

4.1.9 Lattice parameter study:

The **lattice constant**, or **lattice parameter**, refers to the physical dimension of unit cells in a crystal lattice. Lattices in three dimensions generally have three lattice constants, referred to as *a*, *b*, and *c*. However, in the special case of cubic crystal structures, all of the constants are equal and we only refer to *a*. Similarly, in hexagonal crystal structures, a and *b* constants are equal, and we only refer to the *a* and *c* constants. A group of lattice constants could be referred to as lattice parameters. However, the full set of lattice parameters consist of the three lattice constants and the three angles between them.

The lattice parameter of the β-TCP and its doped variants were studied by using XRD. Described by Dickens et al. [3, 4], the beta-TCP crystallizes in the rhombohedral space group R3c with unit-cell parameters, where a = 10.439 Å and c=37.375Å. There are always complexities of determining the lattice parameters ***a,*** and ***α*** of the rhombohedral unit cell. But the measurements of the rhombohedral cell can be determined from the dimensions of the hexagonal cell, and this is an easier process than solving the rather complicated plane-spacing equation for

the rhombohedral system [5]. In this study the unit cell parameters of all the variants are calculated in hexagonal set up.

The parameters of the rhombohedral cell are determined from the following equations:

$\lambda = 2d\sin\theta$ $\lambda = 1.54056$

$aH = 1/3\ \sqrt{[3a^2{}_H + c^2]}$

$$\sin\frac{\alpha}{2} = \frac{3}{2\sqrt{3 + (c/a_H)^2}}$$

$$\frac{1}{d^2} = \frac{4}{3}\left(\frac{h^2 + hk + k^2}{a^2}\right) + \frac{l^2}{c^2}$$

Where Miller indices of a plane are (hkl), a&c are unit cell arm length.

4.1.10 Contact angle study

This is the angle, predictably measured through the liquid, where a liquid–vapour edge meets a solid exterior. This angle is a guidance of the wettability of solid surface. A lesser contact angle means that the material is having water loving and high-energy surface characteristics. But an upper contact angle means that the material possesses water repellent and low-energy surface properties. This study was done by using contact angle analyser Phoenix 300, taking SBF fluid as probe material.

4.1.11 X-ray diffraction (XRD) analysis

X-ray diffraction is an important technique in the field of materials characterization to obtain structural information on an atomic scale from both crystalline and non-crystalline (amorphous) materials. The X-ray diffraction is nondestructive and can be successfully applied to determine crystal structures of metals and alloys, minerals, inorganic compounds, polymers and organic materials as well as to derive such information as crystallite size, lattice strain, surface and interface roughness, chemical composition, and crystal orientation.

X-ray diffraction (XRD) analysis was done for the calcined powder of all the samples i.e. .pure β-TCP powder and its doped variants. The dehydrated calcined (800 °C) powders were pounded into fine powder to break down the powder agglomerates before analysing in an X-ray

diffractometer. Powder samples were positioned in the specimen holder of a Rigaku diffractometer (Model-Miniflex, Rigaku Co., Tokyo, Japan) independently, and then analysed, using Kb filtered Cu Kα radiation in the step scanning mode with tube voltage of 30KV and current of 15mA. The XRD patterns were recorded in the 2θ range of 0-80° with scan speed 1deg/min. All the calcined powders (both pure and doped) were analysed for their phases in the same manner.

4.1.12 Fourier Transform Infrared Spectroscopy:

FT-IR stands for Fourier Transform Infrared spectroscopy, the most preferred method of infrared spectroscopy. In infrared spectroscopy, IR radiation is passed through a sample. Some of the infrared radiation is absorbed by the sample and some of it is passed through or transmitted. An infrared spectrum represents a fingerprint of a sample with absorption peaks which correspond to the frequencies of vibrations between the bonds of the atoms making up the material. Because each different material is a unique combination of atoms, no two compounds produce the exact same infrared spectrum. Therefore, infrared spectroscopy can result in a positive identification (qualitative analysis) of every different kind of material. In addition, the size of the peaks in the spectrum is a direct indication of the amount of material present. Fourier Transform Infrared Spectroscopy (FTIR) refers to a fairly recent development of IR spectroscopy in which the data is collected and converted from an interference pattern to a spectrum.

In this work, we carried out FTIR measurements of the prepared powders to further establish the phases formed due to incorporation of dopants. FTIR measurement were performed in mid IR region (5000-400 cm-1) using KBr pallets in a Perkin- Elmer, Model No- 1615 (USA) instrument.

4.1.13 SEM and EDX study:

Scanning Electron Microscopy was done to investigate the microstructure. The presence of pores and its size, grain size and nature of crystal formation were studied. The sintered pellets of β – TCP and its dopants were broken by a hammer. These broken surfaces were studied under scanning electron microscope .The pore diameters were measured by perfect screen ruler software. Five different SEM images of each sample were taken and their average value was taken for reporting.

In this work, the surface morphology as well as for the microstructure of the dense samples were observed and subsequently assessed for the influence of the dopant ion incorporation during the high temperature process by using a Scanning Electron Microscope (JEOLSEM, Model No-JSM, 5200,TOKYO,Japan). Prior to submission of the samples for SEM analysis, , samples were subjected to polish using polishing machine(LECO Co, JAPAN) to make the surfaces "flat-parallel" for the purpose of better viewing of the microstructures. Gold sputter coating (100 nm thickness) was given to each sample prior the SEM observation.EDX Experiment was done in JSM-7900F Schottky Field Emission Scanning Electron Microscope.

4.2 Mechanical Characterization:

4.2.1 Hardness: Nanoindentation

As our aim is to develop a suitable material that can be used as a bone analogue, we have performed few basic tests to determine the mechanical properties of the materials, like Hardness. Sample preparation for mechanical property evaluation is one of the very important aspects that involve a lot of expertise as well as patience. These samples were then subjected to surface grinding to make both surfaces parallel and then further to "flat paralleling" of the surfaces. After this, the ceramic samples have to be polished for which diamond pastes are used. Initially, lapping is done on a clean glass plate using 10 μm grit size diamond paste and a lubricating oil. After this, the samples are polished in a polishing wheel using 3μm, followed by 1 μm and 0.25 μm grit size diamond paste on a polishing cloth, till "mirror finish" polishing was obtained. Nano indentation is now commonly used for the study of mechanical properties of materials on the nanoscale. Using indentation technique hardness (H) and elastic modulus (E) were measured. When the indenter is pressed into the sample, both elastic and plastic deformation occurs, which results in the formation of a hardness impression conforming to the shape of the indenter. During indenter withdrawal, only the elastic portion of the displacement is recovered, which facilitates the use of an elastic solution in modeling the contact process. Nanoindentation hardness is defined as the indentation load divided by the projected contact area of the indentation. It is the mean pressure that a material can support under load.

In our experimental work, sintered samples were tested by the nanoindentation machine (Fischerscope H100-XYp; Fischer, Switzerland). The depth sensing resolution and force sensing resolution were 0.1nm and 0.2μN, respectively. The machine was calibrated with

nanoindentation based independent evaluation of H ~ 4.14 GPa and E ~ 84.6 GPa of a Schott BK7 Glass following the standards DIN 50359 and DIN EN ISO 14577. The experiments were conducted at a constant load of 100mN with a Berkovich indenter. The Berkovich Indenter had a tip radius of about 150 nm and a semi-apex angle of 65.030. Both the loading and unloading time were 30 seconds.

4.3. Biological characterization:

The biological characterization of biomaterials is of great interest. Living tissue form a thin layer around the inert biomaterial, but materials that irritate the tissues, cause inflammation.

In our study, in vitro and in vivo biological characterization of the composites has been done in details.

4.3.1 In-vitro study:

4.3.1a.Bioresorption Analysis

The fundamental requirement of any biomaterial is the ability of the material to perform effectively with an appropriate host response for the desired application. The body fluid constitutes water, complex compounds, dissolved oxygen and large amounts of sodium (Na^+) andchloride (Cl^-) ions, amino acids, proteins, plasma, lymph, other electrolytes, such as bicarbonate and small amounts of potassium, calcium, magnesium, phosphate, sulphate etc.Additionally, the human body environment is characterized by a salt content of about 0-9% with an average pH of 7.4 and a temperature of 37°C.

As has been frequently reported [4], the SBF is an acellular solution with an ionic composition (in units of mM, 142Na+, 5.0 K+, 1.5Mg^{2+}, 2.5 Ca^{2+}, 103.0 Cl^-, 27.0 HCO_3^-, 1.0 $HPO_4^{2-}$and 0.5 SO_4^{2-}) almost equal to that of human plasma and buffered at a similar pH.

Table 4.1: Ion concentration of SBF in comparison with human blood plasma [6]

Ion	Concentration ($mmol/dm^3$)	
	Simulated body fluid (SBF)	Human blood plasma
Na^+	142.0	142.0
K^+	5.0	5.0
Mg^{2+}	1.5	1.5
Ca^{2+}	2.5	2.5
Cl^-	147.8	103.0
HCO_3^-	4.2	27.0
HPO_4^{2-}	1.0	1.0
SO_4^{2-}	0.5	0.5

Preparation of SBF:

(a) Cleaning:

Cleaning of all the bottles including flasks, beakers etc. with dilute hydrochloric acid solution, sterilizing agent and distilled water is done in the following order:

- All the bottles etc. are immersed in diluted hydrochloric acid solution for several hours. After that they are removed and washed under tap water.
- Then they are immersed in sterilizing liquid for overnight, followed by washing with distilled water.
- After washing, the bottles are covered by wrapping film. If the bottles need to be dried, they are placed in drier below 50^oC.

(b) Dissolution of chemicals:

- 750 ml of distilled water is poured into a 1000 ml beaker (polyethylene beaker is preferred). The water is stirred using magnetic stirrer and the temperature is kept at 37°C with heater. The beaker is preferred to be placed in clean bench, to avoid dusts.
- Each chemical into the water is added one by one in the order given in table, till #8 [Following Table 4.2].
- Addition of reagent #9 [Following Table 4.2] should be little by little with less than about 1g, in order to avoid local increase in pH of the solution.

(c) Adjustment of pH:

- The pH meter with fresh standard buffer solution is calibrated.
- The temperature of the solution in the beaker is checked, and the electrode ofpH meter is placed in the solution. The pH is measured while the temperature is at 37°C. At this point, pH of the solution is approximately 7.5. Titration with 1kmol/dm^3-HCl solution with pipette is done to adjust the pH at 7.25 (or 7.40).
- After the adjustment of pH, the solution is transferred from the beaker to a glass volumetric flask of 1000 ml.
- Distilled water is added to the solution to adjust the total volume of the solution to 1000 ml. The flask is shaked well and kept inside the incubator at 37°C.
- **Table 4.2: Reagents for preparation of SBF (pH 7.25, 1 lt)[7]**

Order	Reagent		Amount
#1	NaCl	Assay min. 99.5%, MERCK,INDIA	7.996 g
#2	$NaHCO_3$	Assay (after drying) min. 99.5-100.3%, MERCK,INDIA	0.350 g
#3	KCl	Assay min. 99.5%, MERCK,INDIA	0.224 g
#4	$K_2HPO_4 \cdot 3H_2O$	Assay min. 99.0%, MERCK,INDIA	0.228 g

#5	$MgCl_2 \cdot 6H_2O$	Assay min. 98.0%, MERCK,INDIA	0.305 g
#6	1 kmol/m^3 HCl	87.28 mL of 35,4% HCl is diluted to 1000 mL with volumetric flask	40 cm^3
#7	$CaCl_2$	Assay min. 95.0%, MERCK,INDIA Use after drying at 120 ^oC for more than 12 hours	0.278 g
#8	Na_2SO_4	Assay min. 99.0%, MERCK,INDIA	0.071 g
#9	$(CH_2OH)_3CNH_2$	Assay (after drying) min. 99.9%, MERCK,INDIA	6.057 g
#10	1 kmol/m^3 HCl	87.28 mL of 35,4% HCl is diluted to 1000 mL with volumetric flask	Appropriate amount for adjusting pH

In order to evaluate the dissolution behavior of the β- calcium phosphate and its doped ceramics in physiological environment, the in vitro dissolution study was carried out by immersing the respective samples simulated body fluid (SBF) solutions.

The rate of bioresorption of the sintered samples was determined in terms of their weight-loss as a function of time, in simulated body fluid (SBF). In this study each sample was immersed separately in 100 ml freshly prepared SBF, kept inside stoppered conical flasks. These were placed inside an incubator at 37°C under static condition. The weight was taken in three alternate days for one month. At the end of each respective day, the samples were taken out from the stoppered conical flasks, dried at 65°C in a hot air oven followed by weight measurement to calculate weight loss/gain as a function of time. In this study, the dissolution behaviour of the samples has been determined by UV_VIS double beam spectrometry (ELICO-177, INDIA).

4.3.1b Hemolysis study

Hemocompatibility is a very important character to decide before the application of any kind of devices or implants such as orthopaedic implants. Very often inside the body the implanted material may come in contact with the blood vessels such as capillary and may induces if the material is not hemocompatible. Therefore it is necessary to improve the hemocompatibility by surface alteration or re-design. When blood contacts with a foreign biomaterial surface, the first event that happens is the competitive adsorption of plasma proteins [8]. Many processes are there to enhance hemocompatibility of biomaterials by surface reform. The improvement of hemocompatibility on a biomaterial surface targets at reducing protein adsorption with the eventual goal of decreasing platelet adhesion. As the TCP coated implants can be an ideal choice in many cases or the use of doped TCP in many bones healing process is becoming common, its hemolysis nature is needed to investigate. In our study we have followed ASTM F756 standard [7] to perform hemocompatibility tests. For each test material 5 pellets were taken and their average OD is taken for the calculation.

In vitro hemocompatibility study was carried out using human blood. Human blood was taken in a Sodium Citrate solution (3.8 gm %) in10:1 ratio and was diluted with normal saline (4:5). Five pellets of each sample (β –TCP and its dopants) as test material (3 gm approximately), without sharp edges were taken in standard test tubes containing 10 ml of (N) saline and incubate at 37^0C for 30 min. 0.2 ml of diluted blood (Blood+ Sodium Citrate solution) were added to each test tube, mixed gently and incubated again for 60 min. One Positive control was prepared by taking 0.2 ml of diluted blood in 10 ml of 0.1% Na_2CO_3 solution and incubated for 60 min at 37^0C. Similarly a Negative control was prepared by adding 0.2 ml of diluted blood in 10 ml of normal saline solution and incubates for 60 min at 37^0C.After incubation, all test tubes were centrifuged for 5 mints at 500g and the supernatant is carefully tested for optical density (O.D), which was measured at 545 nm in a UV-Vis spectrophotometer.

The percentage of hemolysis is calculated from the following equation:

$$\%\ \text{hemolysis} = \frac{\text{O.D.(Test)} - \text{O.D.(Neg.)}}{\text{O.D (Positive)} - \text{O.D.(Neg.)}} \times 100$$

4.3.1c MTT Assay

Peripheral blood mono nuclear cells (PBMC) cells were distributed on 48 well plates for 1 day. Then they were treated with β - tri calcium phosphate and its dopants and incubated for 24 hours. After that MTT was added to each well plate, shaken for 15 minutes and then incubated for four hours. Addition of MTT kill the cells and crystals were formed. Then the media was removed and DMSO was added to dissolve the crystals and a purple coloured solution was formed. The intensity of the colour depends on the amount of crystal formed. When cells died, OD was taken at 545 nm against a blank .The experiment was performed in duplicate and the mean data was recorded.

4.3.1d Bactericidal study

Nutrient agar media was mixed with distilled water in a conical flask. This media was then autoclaved at 121°C for 20 mints to make it sterile. Once this media was cooled down to 40-45°C, the inoculated culture of *Staphylococcus aureus* was mixed with it and distributed to petri dishes (about 22 to 25 ml in each petri dish) and wait for some times to solidify the media. Then the porcelain bit was dripped into the sample under testing. Due to capillary action the sample will come into the bit and they were placed on the Petri dish. Two bit for two types of concentration is taken .In one bit the higher concentration of 2 mg/10ml and in another the lower concentration of mg/10ml were taken and placed on the Petri dish. After complete the sampling all the Petri dishes were kept into the incubator at 30-35°C for 24 hour.

4.3.2 In-vivo study:

Animal experimentation was carried out following the procedures conforming to the standards of the Institutions Animal Ethical Committee of the West Bengal University of Animal and Fishery Sciences, India.

This study was evaluated early stage osteogenesis and bone remodeling in vivo using a critical size defect model in the proximal tibia of New Zealand white rabbits over an 8 week period.

4.3.2a Implant preparation

The manufactured pure and doped crystalline β-TCP powders were pressed at 150MPa for homogeneous densification. All the green specimens were slowly dried at 80°C for 3 days and finally, all the composition were sintered at 1100°C with holding time of 2 hours at that temperature. These samples were then given a cylindrical shape having a dimension of length

6±0.5 mm and 4±0.5 mm of diameter. The samples were initially disinfected by using hot distilled water and consequently autoclaved at 121°C for 30 min before implantation.

4.3.2b Animal experimentation

The present *in vivo* experiments were carried out at West Bengal University of Animal and Fishery Science (WBUAFS), West Bengal, India following the standard protocol and guidelines of the Institutional Animal Ethics Committee (IAEC) of WBUAFS. The permission is given by the "Animal Ethics Committee" (Permit No. Pharma/IAEC/460(v) dated. 04.08. 2016), at West Bengal University of Animal and Fishery Sciences, Kolkata.

In the present study, 14 rabbits of either sex, weighing 2-2.5 kg were randomly distributed into three groups. Two animals were taken in control group I, four animals were taken under the test group II and eight animals were taken under test group III. The animals were housed indoor in standard conditions, free to move according to the guidelines of Institutional Animal Ethical Committee of the West Bengal University of Animal and Fishery Sciences, India. Surgery was performed under aseptic conditions and sedation by injection of Xylazine hydrochloride (XYLAXIN®, Indian Immunologicals, India) at a dose of 1 mg/kg body weight and Ketamine hydrochloride (Ketalar®, Parke-Davis, India) at a dose of 25 mg/kg body weight intramuscularly. A bone defect (5 mm × 2.5 mm × 3 mm) in all the animals was created in the femoral condyle with the help of a motorized dental drill (Fig1). In all the animals, implants were secured in position by suturing muscle, subcutaneous tissue and skin in layers. All the treated animals were administered Cefotaxime sodium (Mapra India,India) at a dose rate 125 mg/kg of body weight intramuscularly, at 12 h interval daily for 5 days and Meloxicam (MELONEX®, Intas Pharmaceuticals, India) at 0.2 ml once daily for 5 days. Surgical wounds were dressed daily with Povidone iodine and antibiotic ointment for 10 days post-operatively.

Figure 4.1. Steps of creating bone defect and implantation.

For group I animals (control) no sample or no load is applied in the defected site. For group II animals TCP and Ti doped TCP samples are implanted separately but no load is applied. For group III animals TCP and doped TCP with Zn, Mg and Ti samples are implanted separately .After 7 days post operatively, the first dynamic loading (in the form of axial oscillatory vibration) was applied to all the animals presented under group III. The idle span of seven days was kept as to ensure a steady callous formation as a function of time. Afterwards vibration was given twice a week at a frequency of three cycles per second for a total span of 40 minutes with the help of a simple set-up **(Figure 4.2),** developed by us. Prior to the application of loading, all the animals were anaesthetized. The legs with implant, put into the site, were fastened flawlessly so that the applied load by the machine can be rightly functional to the implanted bony part. The applied load was given in a uniform magnitude and uniform frequency. A study of one month and two months duration was done.

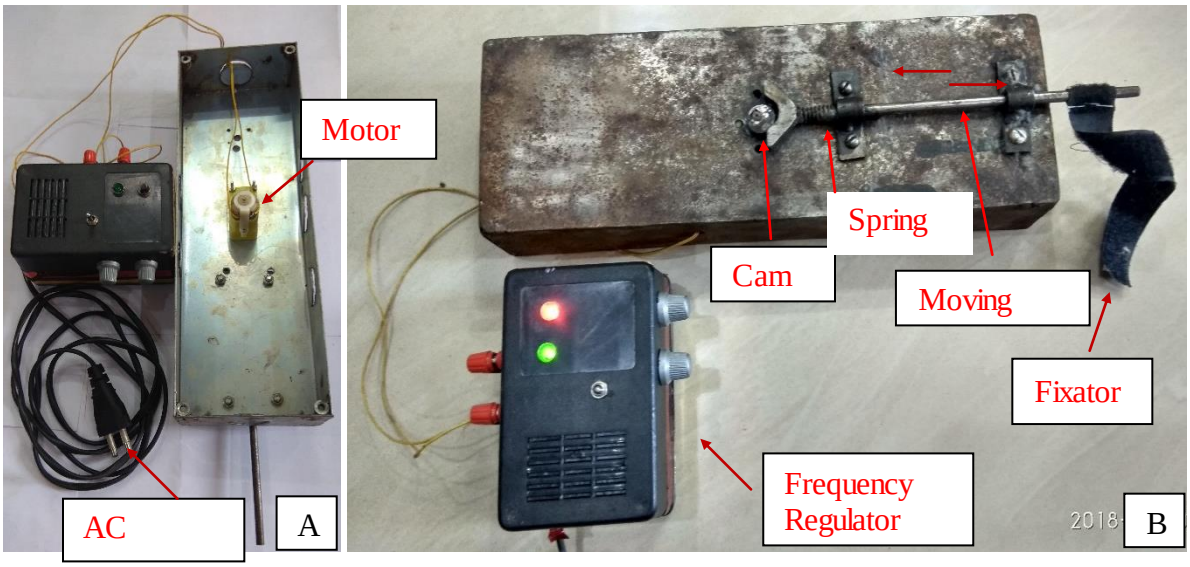

Figure 4.2: The machine which was used to produce axial oscillatory vibration.

A. Inside B. Outside

Description: 1.Motor: 150 Dual Shaft straight Gear motor

2. Cam: made of Stainless stell

3. Power: AC supply (250 Volt,50Hz)

4.3.2c Local inflammatory reaction and healing of wound

Lameness, inflammation, seroma formation, edema, hematoma, and associated signs of local inflammatory reactions were observed post operatively from the day 1 and changes were evaluated by visual and manual examinations.

4.3.2d Radiological examination

Radiographs were taken immediately after implantation and subsequently on days 30, 60 postoperatively of the operated area. Radiographs were observed for the status of implant, host-bone reaction to implant and new bone formation.

5.3.2e Micro-computed tomography

In this study, the critical size bilateral bone defects of size 6 mm X 4 mm were created. Sterilized pure TCP and Zn, Mg and Ti doped TCP were implanted in the bone defects. After 1month (1M) and 2 month (2M) the animals were euthanized and femurs were removed and stored in 10% formalin. The post operated formalin preserved bone samples were analyzed using micro-CT (Phoenix V|tome|xs, GE,Germany). Prior to the analysis, all the bone samples were dried in room temperature. All the bones were scanned at a voltage of 80 kV and a current of 75 µA. Time fraction was 500 ms per image with 1000 images in one complete rotation. The voxel size is fixed as 18 µm. No filter was applied. The constructed 2D images were compiled to build 3D models using VG studio MAX 2.2.

4.3.2f. Histological study

The implanted ceramic implants along with the surrounding bones were collected from the animals at day 30 and 60 postoperatively. The sections from both normal and implanted area were cut (3–4mm thick) using hack saw and washed thoroughly with normal saline and were fixed in 10% formalin for 7 days. Subsequently, bones were decalcified in Gooding and Stewart's fluid containing formic acid 15 ml, formalin 5ml and distilled water 80 ml solution. The decalcified tissues were processed in a routine manner and 4 µm sections were cut and stained with haematoxylin and eosin. The stained sections were observed for status of the bone implants and cellular response of host bone to the implants.

4.3.2 g.Oxytetracycline labelling study

Fluorochrome (oxytetracycline dehydrate; Pfizer India, India), at a dose of 25 mg/kg body weight, was given before sacrificing the animals. Undecalcified ground sections were prepared from the implanted segments of bone and the sections were ground to 20 µm thickness using different grades of sand paper. The ground undecalcified sections were observed under ultraviolet incidental light with an Orthoplan microscope (Excitation filter, BP-400 range, Leitz, USA) to analyze bone formation within the implants.

4.3.2h SEM images of Bone implant interface

New bone formation on and surrounding the implant was verified by detailed SEM study (ZEISS, EVO system) at the end of study of 30 and 60 days. After removing the soft tissue, the implanted bone specimens were fixed in 5% glutaraldehyde phosphate solution, washed twice for 30 min with phosphate-buffered saline (pH7.4) and distilled water and then dehydrated in a series of graded alcohol solutions. Finally samples were dried with hexamethyldisilizane. A gold conductive coating was applied (gold-palladium alloy for 120 seconds) by ion sputtering (JEOL ion sputter, model JFC 1100, Japan) at 7–10 mA and 1–2 kV for 5 min. The resin-mounted sample surfaces were then examined under SEM after proper alignment to understand the orientation and distribution of newly formed osseous tissues and distribution/absorption of materials at the defect site.

References

[1] American Society for Testing and Materials, C830-00: standard test methods for apparent porosity, liquid absorption, apparent specific gravity and bulk density of refractory shapes by vacuum pressure, ASTM Annual Book of Standards, Volume 15.01:Refractories; Activated Carbon; Advanced Ceramics (2002)

[2] R.W. Grimshaw, The Chemistry and Physics of Clays and Allied Ceramic Materials, fourth ed., Wiley, New York, 1971.

[3]. Dickens B, Schroeder L.W, Brown W.E, *J. Solid State Chem*.10 232–248, 1974.

[4]. Schroeder L.W, Dickens B, Brown W.E, *J. Solid State Chem*.22 253–262, 1977.

[5]. Cullity B.D. *Elements of X-ray Diffraction*, 2nd Edition, Morris Cohen (California; Addison-Wesley Publishing Company Inc.) pp 504-505

[6] Kokubo T, Takadama H. How useful is SBF in predicting in vivo bone bioactivity? 569 Biomaterials 27: 2907–15, 2006.

[7] A. Oyane, H.-M. Kim, T. Furuya, T. Kokubo, T. Miyazaki and T. Nakamura,"Preparation and assessment of revised simulated body fluid", J. Biomed. Mater. Res., 65A, 188-195, 2003.

[8] American Society for Testing and Materials - ASTM. ASTM F-756: standard practice for assessment of hemolytic properties of materials. West Conshohocken; 2000.

CHAPTER: 5

RESULTS & DISCUSSIONS

RESULTS AND DISCUSSIONS

This chapter is divided into different sections as listed below.

1. Development of pure and doped β-TCP and their physical characterization.
2. Mechanical Characterization of pure and doped β-TCP
3. Biological Characterization of pure and doped β-TCP
4. In Vivo Characterization of pure and doped β-TCP

1. Development of pure and doped β –TCP and their physical characterization:

5.1.1 X-ray diffraction data

X-ray diffraction data of the β-TCP powder and of all doped compositions calcined at 800ºC temp. were recorded in 2θ range. The obtained XRD patterns of pure β-TCP and β-TCP powder doped with 3 wt. % and 5 wt. % samples were presented in figure 5.1 and 5.2 respictively. The pure powder calcined at 800 ºC developed several high intensity peaks corresponding to various planes i.e. (1 0 10), (2 1 4), (0 2 10) and (2 2 0) ,(2 0 20) as revealed by study, with reference PDF card No.- 09-0169 for β-TCP. The XRD patterns of the pure β-TCP and doped powders calcined at 800ºC clearly explain the presence of the most prominent peak at 2θ angle of ~31.026º, corresponding to (0 2 10) plane. Presence of this sharp peak suggests that crystallites of β-TCP phase were formed as a result of calcinations at 800ºC. Almost similar patterns were recorded for all these compositions, which suggest that the presence of 3 wt.% and 5wt.% dopants did not alter the phase purity of crystalline β-TCP.

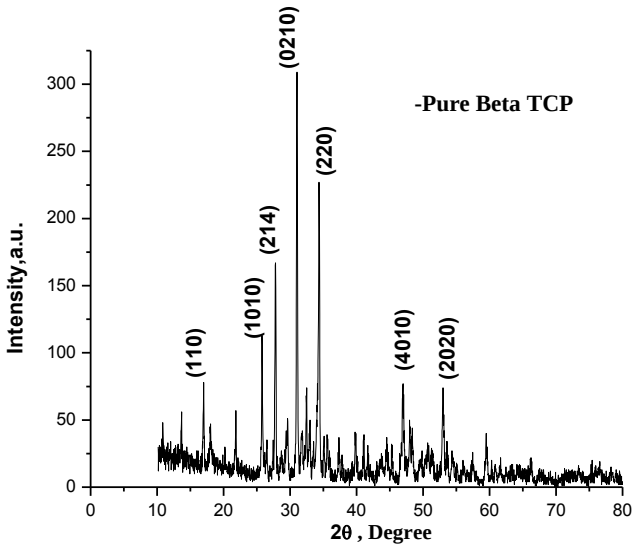

Figure 5.1: XRD pattern of pure β-TCP

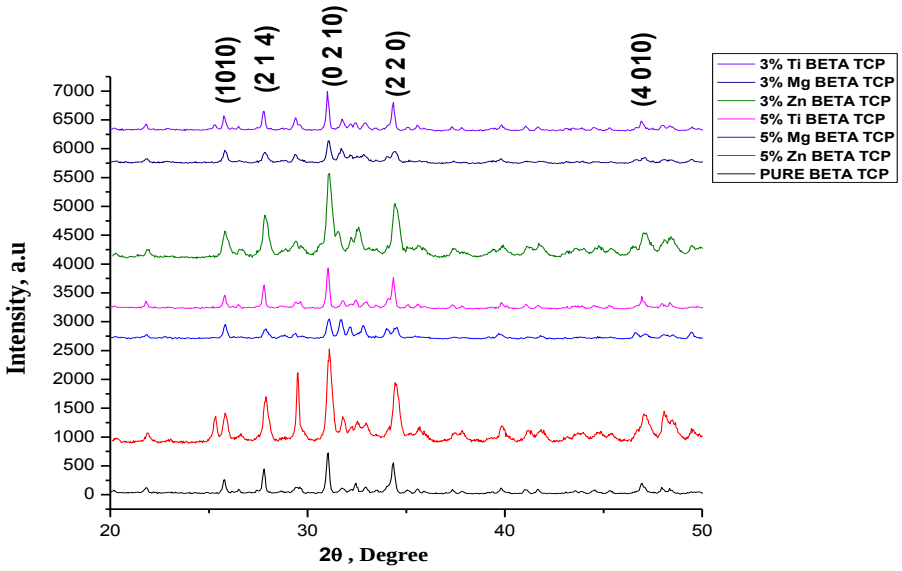

Figure 5.2: XRD pattern of β-TCP along with its doped Variants

5.1.2 Lattice parameter study

The lattice parameters suffered minor changes due to the incorporation of different dopants. The values of both a and c axis decreased systematically in all the cases, shown in below table 5.1. This may be attributed to smaller atomic radii of the dopants e.g. Zinc (134 pm), Magnesium (160 pm), and Titanium (147 pm) in comparison with Ca (197 pm). The results confirmed the substitution of calcium ion by the dopants and consequent reduction in unit cell dimensions.

Table 5.1: Result of Lattice parameters

Sl.no	Compositions	a axis (Å)	c axis (Å)
1	Pure β-TCP	10.47	37.37
2	5% Zn- β-TCP	10.38	36.26
3	5% Mg-β-TCP	10.43	37.17
4	5% Ti-β-TCP	10.41	36.96

5.1.2 FTIR Analysis

The obtained FTIR patterns of pure β-TCP and doped β-TCP powder were presented in the figure 5.3 and 5.4 respectively. In this FTIR plot of pure calcined β-TCP powder we got prominent sharp peak at 3575 which indicates the presence of hydroxyl group. In some cases these

hydroxyl group peak is very short and tending to disappear. This may due to the evaporation of the surface moisture of the powder. The peaks at 607 and at 1045 are due to the presence of phosphate group and a peak at 1470 shows some unreacted carbonate. In case of different dopants more or less the same peaks appeared at almost same locations however there was a slight variation in their intensities.

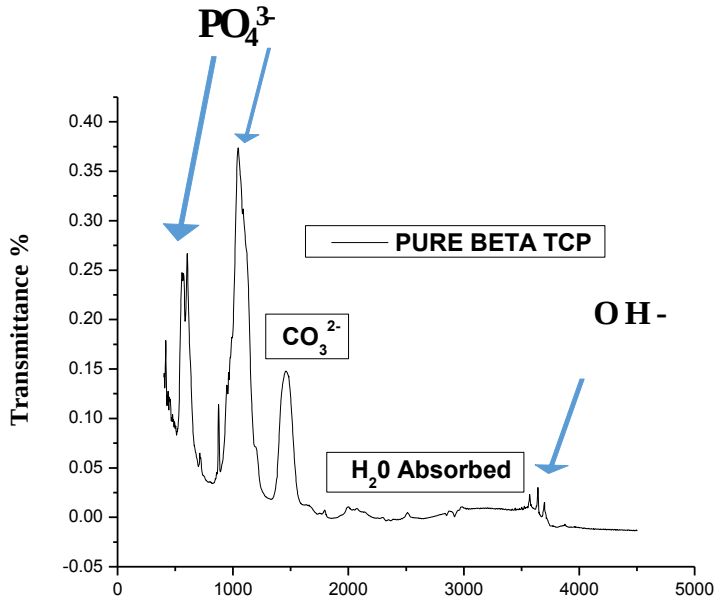

Figure 5.3: FTIR spectra of pure β-TCP

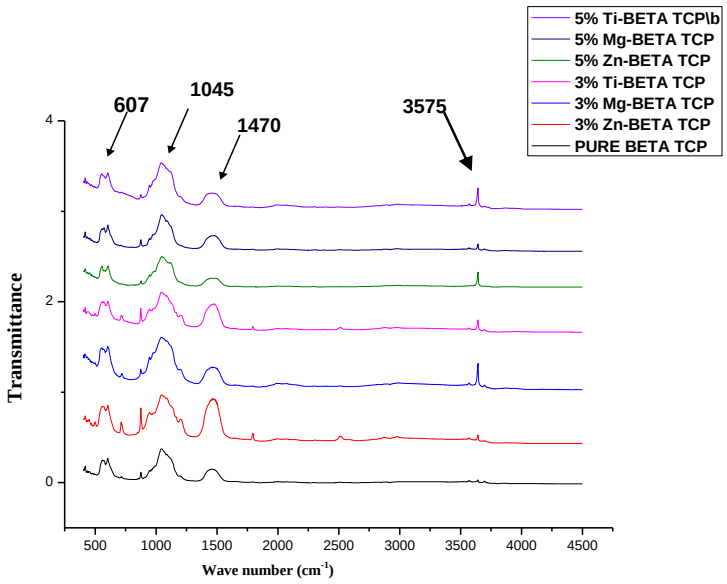

Figure 5.4: FTIR spectra of β-TCP along with its doped Variants

5.1.3 Green density of pure β- TCP and its derivatives

There was as such no significant variation of the green density of different compositions, which suggests their similar kind of bulk volume. Result of this measurement is presented in below table .5.2.

Table 5.2: Green density of pure β- TCP and its derivatives

Sl.No.	Compositions	Green Density (gm./cc)
1	Pure β-TCP	1.52± 0.0207
2	3% Zn - β-TCP	1.54±0.0223
3	3% Mg -β-TCP	1.48±0.0444
4	3% Ti - β-TCP	1.53±0.0240
5	5% Zn -β-TCP	1.55±0.0296
6	5% Mg - β-TCP	1.47±0.0426
7	5% Ti- β-TCP	1.54±0.0303

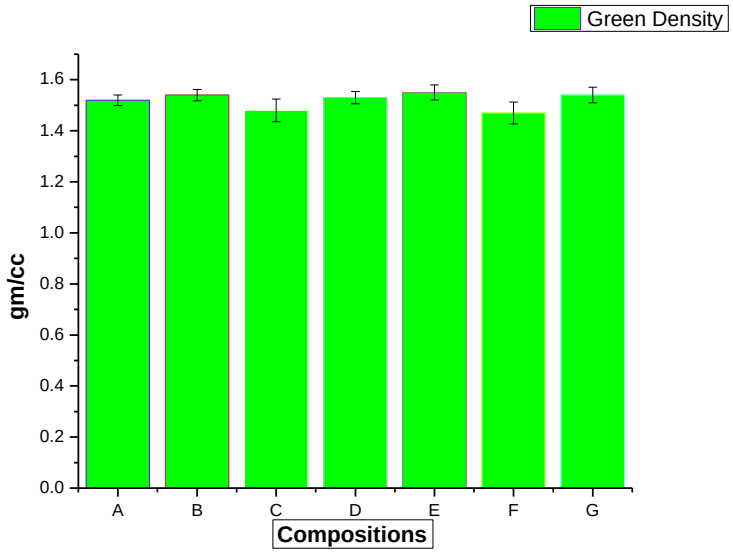

Figure 5.5: The average green density of all compositions (n=5).

A)β-TCP B) 3% Zn-β-TCP C) 3% Mg- β-TCP D) 3% Ti- β-TCP E) 5% Zn- β-TCP F) 5% Mg- β-TCP G) 5% Ti - β-TCP .

This plot depicted that green density of each compositions is near equals to same in order.

5.1.4 percentage of diametric and linear shrinkage at different temperatures

The diameters of all green specimens were 10±0.03 mm and thickness 6±0.03 mm. After sintering average diameter of sintered specimens was 8±0.05 mm and thickness 5±0.05mm. All the pellets of different compositions were measured for its diametric and linear shrinkage with a digital vernier scale. Percentage of diametric and linear shrinkage at different temperatures are shown in below table 5.3.

Table5.3: Percentage of diametric, linear and volumetric shrinkage at different temperatures.

Compositions	%Diametric shrinkage		% Linear Shrinkage	
	1000°C	1100°C	1000°C	1100°C
Pure β-TCP	19.33	19.47	21.66	21.84
3% Zn-β-TCP	19.44	19.56	21.83	22
3% Mg-β-TCP	19.33	19.50	21.82	22.01
3% Ti-β-TCP	19.30	19.31	21.62	21.67
5% Zn-β-TCP	19.4	19.61	22.01	22.8
5% Mg-β-TCP	19.32	19.48	21.07	21.20
5% Ti -β-TCP	19.28	19.30	21.58	21.63

From this result it is evident that at At 1100°C the amount of shrinkage is little bit higher than the At 1000°C. The amount of shrinkage is maximum in case of Zinc doped samples. , possibly due to the densification properties of Zinc in ceramic matrix [1].

Major observations

- **From XRD, it was observed that the phase pure β-TCP powder have been developed for this present study.**
- **The effect of dopants in to lattice parameter was noticed.**
- **FTIR result confirmed about the presence of functional group PO_4^{3-}**
- **Some unreacted CO_3^{2-} also present as observed from FTIR .**
- **FTIR for all compositions remained same, this means to have all functional group of Beta β-TCP .**
- **Green density of the pellets were almost 1/3rd of Sintered density.**
- **Sintering at high temperature increased the density of pellets.**
- **All kind of Shrinkage of specimens increased with increasing temperature .**

5.1.5 Apparent porosity:

Porosity in ceramic biomaterials is very much important in many aspects. If the material is supposed to apply for the load bearing application then the porosity must be low otherwise failure may come soon. If the material is meant for fracture healing like in case of TCP, the significant amount of porosity is very much required. Fine pores create a large surface area which induces high bioactivity. All the inter connected pores can provide a frame work for bone growth. Many time these materials (TCP, its derivatives) are used as a surface coating in implants. The presence of pores in this material helps to build a strong bond between the tissue and implant and also thus help to prevent the micro motion, which in turn increases healthy bone growth. From our result we can understand that the significant amount of porosity is there and it is somehow temperature dependent. If we increase the sintering temperature the porosity is becoming less, because of the evaporation of the residual water in the matrix and hence more compaction and less porosity. The result of the apparent porosity is given in the table 5.4.

Table 5.4 Apparent porosity at different temperatures

Sl.No.	Compositions	At 1000°C (%)	At 1100°C (%)
1	Pure β-TCP	27.54±6.10	16.76±3.98
2	3% Zn-β-TCP	34.68±8.19	27.06±6.75
3	3% Mg- β-TCP	31.03±4.10	22.29±5.39
4	3% Ti- β-TCP	30.04±5.52	26.01±5.49
5	5% Zn -β-TCP	32.26±7.61	30.16±5.97
6	5% Mg -β-TCP	28.09±5.06	26.58±7.19
7	5% Ti- β-TCP	28.32±5.60	26.18±8.11

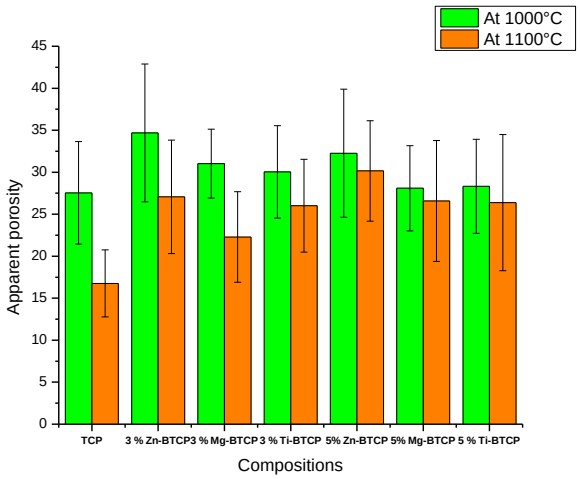

Figure 5.6: Bar diagram of apparent porosity at different temperatures (n=4).

This data clearly shows that porosity is reduced at 1100°C than 1000°C.The 5 % Zinc doped sample is showing the maximum porosity of its category and all the doped samples are showing higher porosity than pure β-TCP. Further it can be said that all the 5% doped variants are showing lesser porosity of its own 3% doped variants.

5.1.6 Grain size, Pore size determination:

The pore sizes are measured by perfect screen ruler software like average grain size measurement. We have analyzed five random SEM pictures of each sample, all of same magnification and the result is shown in table 5.5.

Table 5.5: Grain Size and pore size

Sl.No.	Compositions	Grain Size (nm)	Pore Size(nm)
1	Pure β-TCP	571± 22.49	132±23.71
2	3% Zn-β-TCP	539± 18.71	122±24.67
3	3% Mg-β-TCP	551±21.91	174±22.25
4	3% Ti-β-TCP	547±29.31	157±18.90
5	5% Zn-β-TCP	541±26.10	128± 15.71
6	5% Mg-β-TCP	569±27.95	186±20.24
7	5% Ti-β-TCP	561±21.04	161± 21.21

Grain size as we observed here. Pure β-TCP is having the largest grain size 571nm and the 3 % Zn doped sample is showing the smallest grain size 539 nm.The pore size is smallest in case of 3% Zn doped β-TCP and the 5 % Mg doped β-TCP has the largest pore size. Zn doped samples of all category are showing smallest grain size.

5.1.7 Contact angle study:

The observation by using contact angle analyser Phoenix 300 using SBF as probe material showed that all the specimens are having a contact angle in between 40±4 º. The result is expressed in the following table 5.6.

SBF is hydrophilic in nature. If a material possesses a lesser contact angle with SBF it means that the material is having water loving and high-energy surface characteristics. It gives better wettability, it helps to draw biological fluids to the surface of implants. Our data revealed a lower range of contact angle for each composition. This means that all the samples are truly hydrophilic with SBF and can draw biological fluid in vivo.

Table.5.6. Contact angle study results

Sl.No	Composition	CA(M) [deg.]	CA(L) [deg.]	CA(R) [deg.]
1	Pure β-TCP	32.725	32.24	33.21
2	3% Zn doped β-TCP	32.485	33.9	31.07
3	5% Zn doped β-TCP	33.855	34.21	33.5
4	3% Mg doped β-TCP	29.21	28.4	30.02
5	5% Mg doped β-TCP	32.75	32	33.5
6	3% Ti doped β-TCP	35.15	35.72	34.58
7	5% Tidopedβ-TCP	29.725	30.2	29.25

5.1.8 SEM-EDX study:

The SEM images of all the samples are shown in **Fig.5.7 and Fig.5.8**.These pictures reveal that there are sufficient pores in the samples which can promote bony ingrowth. It also reveals that these materials with structural integrity can act as very good scaffold materials. The grains are predominantly nodular in shape .Elemental analysis revealed that doping agents like Zn, Mg and

Ti are there on the surfaces of the corresponding samples. All the EDX images showed the peaks of the corresponding doping agents.

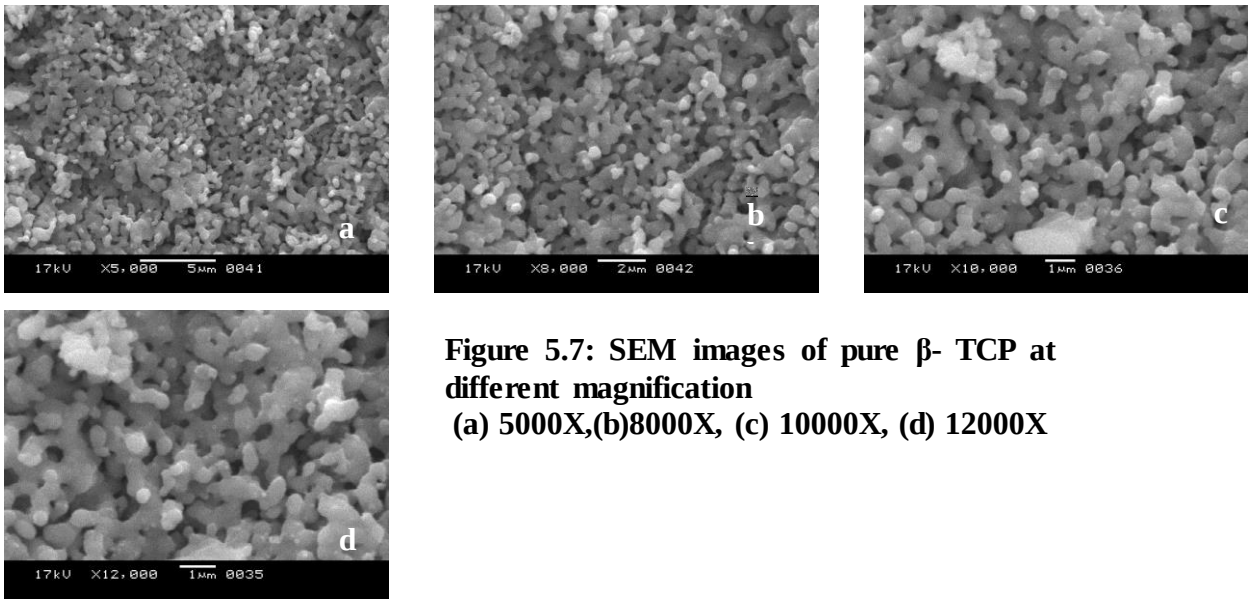

Figure 5.7: SEM images of pure β- TCP at different magnification
(a) 5000X,(b)8000X, (c) 10000X, (d) 12000X

SEM images of doped samples:

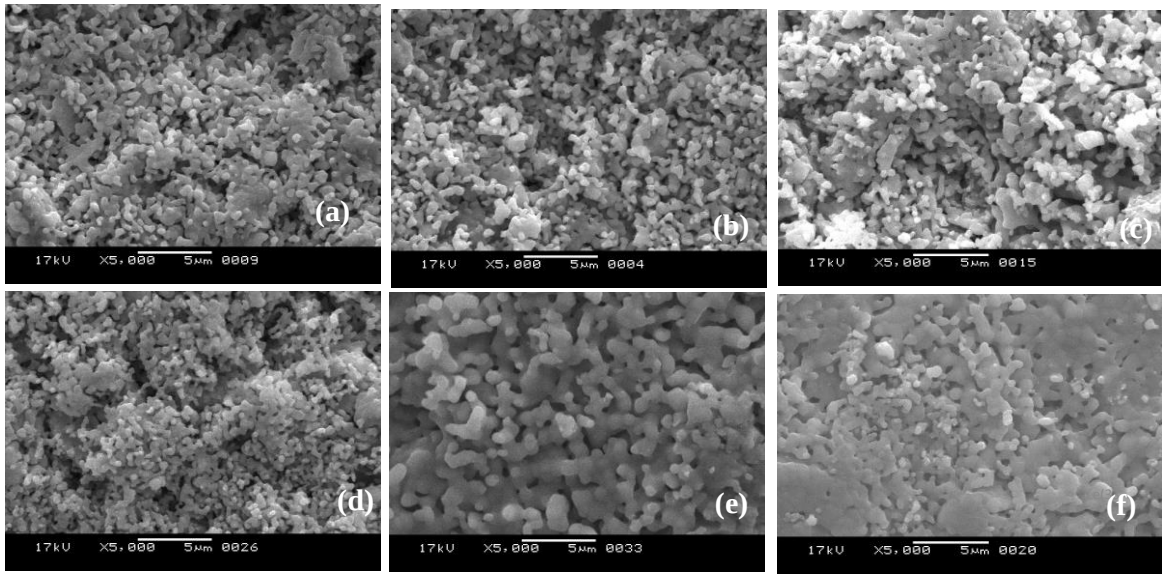

Figure 5.8: SEM images of doped samples: (a) 3% Zn-β- TCP , (b) 3% Mg-β-TCP, (c) 3% Ti- β-TCP, (d) 5% Zn- β-TCP, (e) 5% Mg-β-TCP, (f) 5% Ti-β-TCP

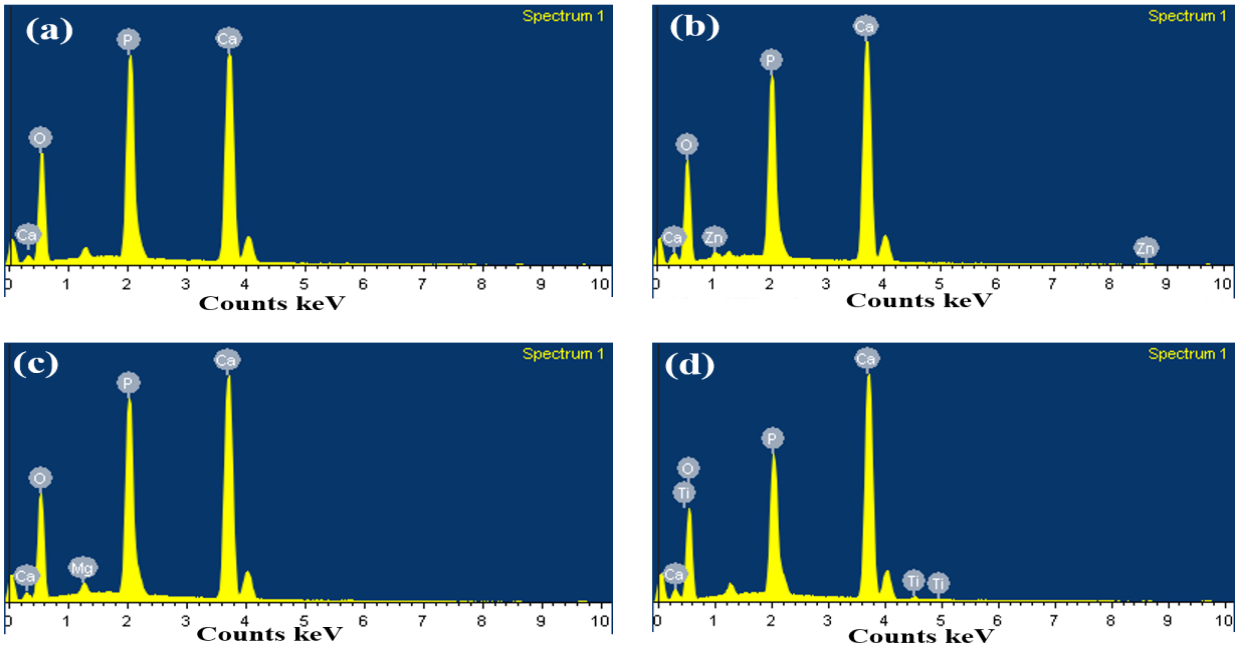

Figure 5.9: EDS pattern of pure and 5 % doped β-TCP, sintered at 1100° C(a) Pure β-TCP (b) Zn-β-TCP (c) Mg -β-TCP (d) Ti -β-TCP .

2. Mechanical Characterization of pure and doped β –TCP:

5.2.1 Hardness at Temperature 1100°C

Our study revealed that the hardness value of β-TCP can be improved by incorporation of dopants to some extent. This may be due to the densification of the ceramic matrix. But there is no proportional relation between the dopant amount and hardness.

Table 5.7: Hardness value

Sl no	Composition	Hardness (GPa)
1	Pure β-TCP	0.652±0.046
2	3% Zn- β-TCP	0.693±0.027
3	3% Mg- β-TCP	0.681±0.076
4	3% Ti- β-TCP	0.665±0.046
5	5% Zn- β-TCP	0.704±0.038
6	5% Mg- β-TCP	0.687±0.094
7	5% Ti- β-TCP	0.672±0.082

The 5% Zn doped β-TCP is showing the maximum hardness value of 0.704 GPa. It may be due to the higher densification of the ceramic by zinc than other ions in the compositions.The observed hardness value is quite similar with the literature value [1].The hardness of all doped compositions is higher than pure β-TCP value.

3. Biological Characterization of pure and doped β –TCP

5.3.1 SBF study:

Scanning Electron microscopy images show formation of apatite layer on each pellet of different quantum after 30 days. We observed that after immersion in the SBF solution, the porous apatite layers formed after 7 days. The samples started to form these porous layers after this period. The SEM images (shown below) after30 days of immersion for all samples showed highly dense apatite layers. The size and thickness of calcium phosphate layers was getting increase with increasing SBF immersion time.

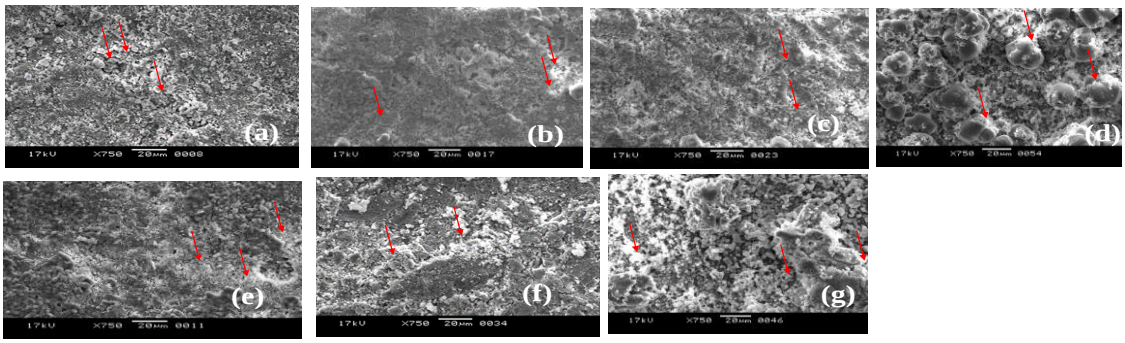

Figure 5.10: SEM images of apatite: (a) β- TCP (b) 3%Zn-β- TCP (c) 3% Mg-β-TCP (d) 3% Ti- β-TCP (e) 5% Zn- β-TCP (f) 5% Mg-β-TCP (g) 5% Ti-β-TCP

5.3.2 Weight degradation. Due to dissolution in the SBF the pellets were gradually losing its weight. We observed a study for 30 days. In each three alternate day we took out the sample from the SBF and gently dry them in air and weighed. The % of weight degradation is expressed in the below figure 5.11.We noticed a rapid loosening of weight in the beginning days up to days 12-15, after that the grade of the dissolution becoming slow. The slow degradation of the pellets may be due to the onset of apatite layer on the pellets.

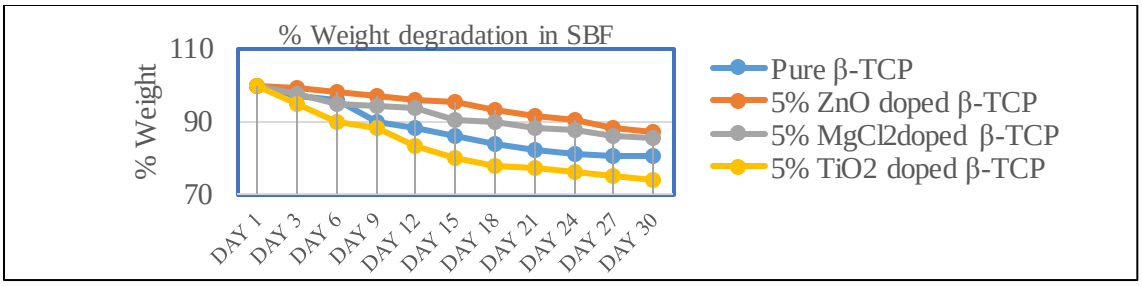

Figure 5.11: Plot of percentage weight degradation in SBF with days.

5.3.3 Percentage transmittance of SBF:

The dissolution of the samples in the SBF was fast at the beginning and gradually became slow with time, which is also confirmed by the percentage weight degradation of pellets in the SBF. Up to 15 days there was a gradual and maximum change for all samples. After this the transmittance became almost stable. This also confirms that as the apatite layer is in the formation process. It stops the leaching out of the materials in to the solution as days go. The following bar diagram shows the percentage transmittance of SBF fluid in different days.

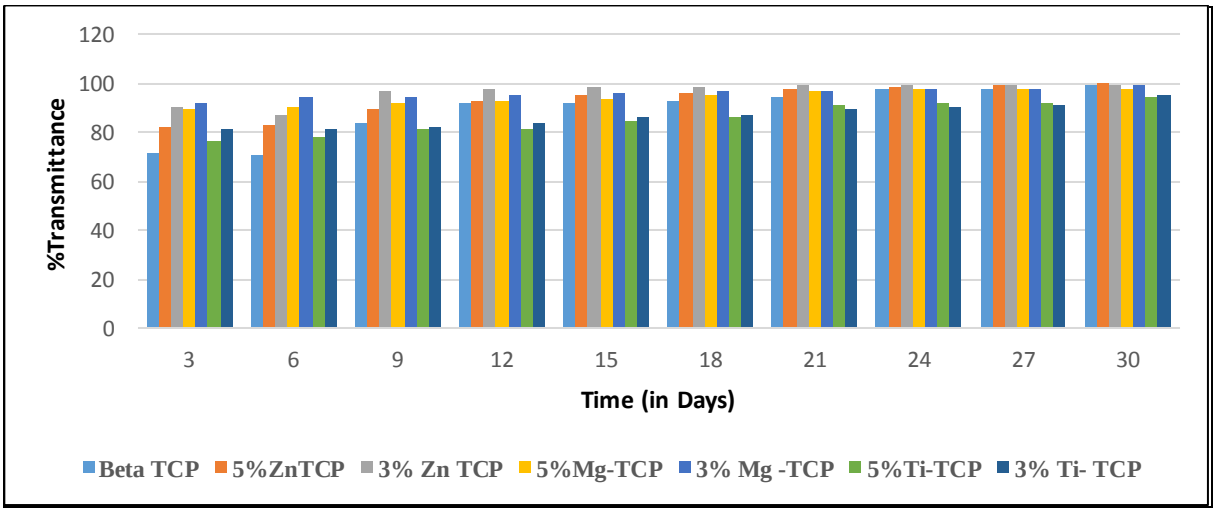

Figure 5.12: Plot of transmittance percentage of β-TCP and its dopants of SBF solution.

5.3.4 Haemolysis study:

Hemocompatibility is an important parameter to be decided for an implant. In our study we have followed ASTM F756 standard to perform hemocompatibility test. For each composition five pellets were taken and their average OD (of 3 observations) was taken for the calculation. One such data set for one observation is given below table 5.8.

Table 5.8: Hemolysis observation data for all compositions

Sl. no	Composition	Wave length (nm)	Avg. O.D. of Test sample	O.D. (+) ve control	O.D. (-) ve control	%Haemolysis
1	Pure β-TCP	545	0.071	0.46	0.061	2.50
2	3% Zn-β-TCP		0.074			3.25
3	5% Zn-β-TCP		0.075			3.50
4	3% Mg-β-TCP		0.078			4.26
5	5%Mg-β-TCP		0.075			3.50
6	3% Ti-β-TCP		0.072			2.75
7	5% Ti-β-TCP		0.073			3.00

Five such different data sets were prepared for five pellets and from there the average hemolysis data is presented in the following table 5.9.

Table 5.9: Data for hemolysis analysis.

Sl.No.	**Compositions**	**%Haemolysis**
1	Pure β-TCP	2.82±0.20
2	3% Zn- β-TCP	3.43 ±0.34
3	3% Mg- β-TCP	4.10 ± 0.43
4	3% Ti - β-TCP	2.97 ± 0.21
5	5% Zn - β-TCP	3.50 ± 0.46
6	5% Mg - β-TCP	3.74 ±0.38
7	5% Ti- β-TCP	3.15 ±0.20

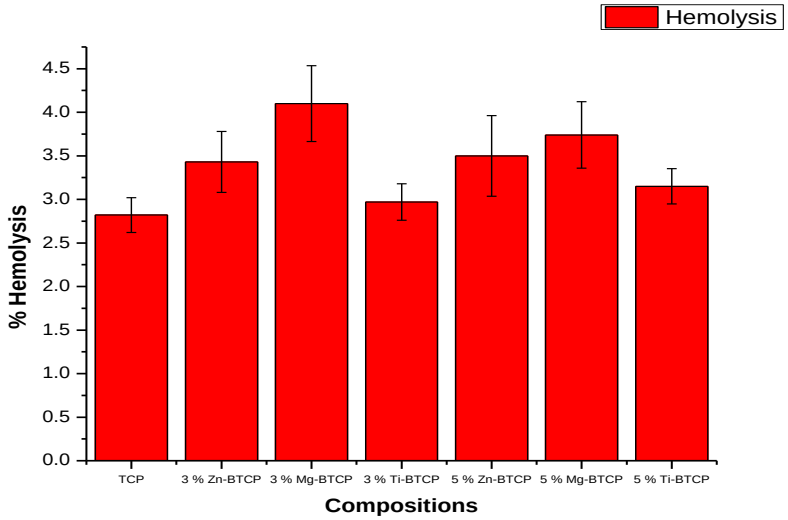

Figure 5.13: Bar diagram of % Hemolysis. (n=5).

As we observed here the % hemolysis of all compositions are falling below 5% level. This ascertain about the highly hemocompatibility nature of all variants according to the ASTM guideline.Among the different compositions pure β-TCP is showing the maximum hemocompatibility .

5.3.5 MTT Assay: The average of % cell Viability as recorded are expressed in the below bar diagram taking n=2.

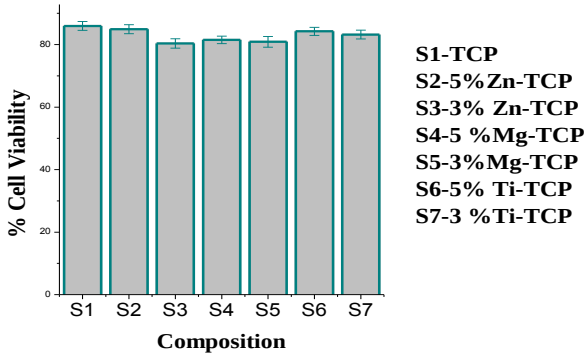

Figure 5.14: % cell viability as observed in MTT assay.

All the samples are showing more than 80% cell viability. These conclude that all these samples are non- cytotoxic in nature.

5.3.6 Bactericidal study:

Antimicrobial activities of any material are understood by its degree of growth inhibition of microorganisms. The pictures of the studied Petri dish are shown in the figure 5.15.

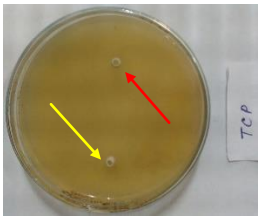

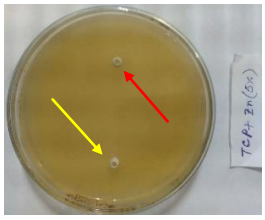

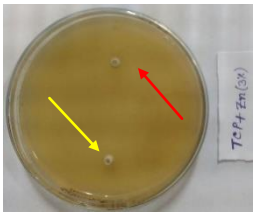

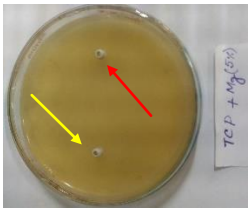

Fig5.15a:β-TCP Fig5.15b:5%Zn-β-TCP Fig5.15c:3% Zn-β-TCP Fig5.15d: 5% Mg-β-TCP

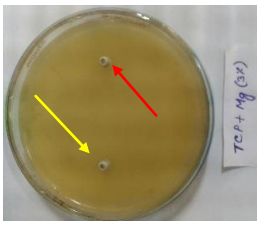

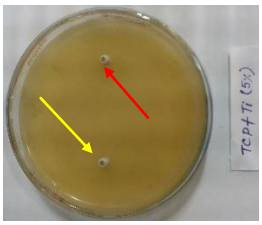

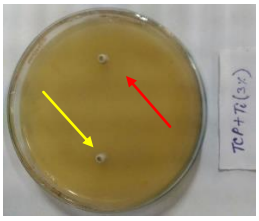

Red and yellow arrow indicate the porcelain bit of having 2mg/10 ml &1 mg/10ml of composition respectively

Fig5.15e.3%Mg-β-TCP Fig: 5.15f.5%Ti-β-TCP Fig:5.15g.3% Ti-β-TCP

We observed no zone of inhibition in either concentration in any petri dish after 24 hour. This suggests that in this concentration (1mg/10ml &2 mg/10 ml) TCP and its dopants possess no bactericidal property.

Major observations

- **Porosity was highly decreased with increasing temperature.**
- **Hardness of all doped compositions was better than Pure β-TCP.**
- **Contact angle data revealed the hydrophilicity characteristics of all specimens.**
- **Uniform microstructure and interconnected pores were observed from SEM analysis.**
- **The EDX spectra confirmed the penetration of dopant ions into β-TCP.**
- **SBF study showed the formation of apatite layer on sintered specimens.**
- **Ti doped composition showed maximum apatite layer formation.**
- **All the specimens are highly hemocompatible.**
- **MTT assay and bactericidal study showed the nontoxic nature of all**

4. In Vivo Characterization of pure and doped β –TCP:

Depending on physical properties and other results on in vitro studies - it may be concluded that 5% doped specimens revealed better results in few important aspects-like high porosity, high quantum of apatite layer formation. These two factors along with the constriction related to the number of animals permitted for animal trial, we decided to go for 5% doped specimens only to conduct detailed animal study. In this context it may be noted that the ethical committee formed as per the law of the land give the permission for animal trial and also fix the no. of animal to be used.

For group I (Contrl) and group II no loading effect is given and after 7 days the first dynamic loading (in the form of axial oscillatory vibration) was applied to all the animals presented under group III, twice weekly at a frequency of 3 per second for 40 minutes with the help of a machine which was discussed under materials and methodology part. (Chapter no: 4).

5.4.1 Local inflammatory reactions and healing of wound:

No marked inflammatory reactions were observed in both the control and experimental group following placement of bioceramic implant up to 60^{th}day postoperatively. There was no adverse local effects such as marked hematoma or oedema during the early postoperative period.

The implants were clinically stable in the bone. No foreign body response or toxicity was elicited and hence it was confirmed that the implant was accepted as a suitable alternative bone graft to fill the defect.

5.4.2 Radiological observations:

5.4.2.1 Group I (control study):

In control animals (empty defect), the radiograph at '0' day showed circular defect in distal metaphysis of femur bone and the defect is still visible at one month(1M) except reducing the diameter of the bone defect. At two (2M) month the radiograph showed further reducing the defect diameter although total gap was not obliterated.

5.4.2.2 Group II (Tri-calcium phosphate dopants without loading effect):

Only pure β-TCP and 5% Ti-doped β-TCP are implanted in this group.

For pure beta β-TCP the 0 day radiograph showed presence of radiodense implants at the distal epiphysis of femur. The implant was observed occupying the defect area but somewhat protruding out the cortical lining. At 1 M, the defect area appeared to be condensed and length of the implant also emerged slightly decreased. At 2 M, the radiodense implant was further reduced in size. The cortical lining over the defect was in the process of bridging of the periosteal lining.

For Ti- β-TCP the "0" day skiagram showed presence of radiodense cylindrical implants tightly filling the defect space at the distal epiphysis of femur. At 1 M, the implant size was reduced and initiation of bridging of periosteal lining in the defect area the discontinued cortical lining as observed on day '0' was almost not visible at 2 M. The size of the implant was further reduced at this stage indicating advanced stage of bridging of periosteal line.

Control **β-TCP- NV*** **Ti-β-TCP- NV** **β-TCP- WV**** **Ti-β-TCP- WV** **Mg-β-TCP- WV** **Zn-β-TCP- WV**

Figure 5.16: Radiographs of the '0' day: *NV: No Vibration (Group-II), **WV: With Vibration (Group-III)

5.4.2.3 Group III (Tri-calcium phosphate dopants with loading effect):

Pure β-TCP and 5 % Zn , Mg and Ti-doped β-TCP are implanted in this group.

The radiograph of pure TCP implanted bone showed presence of radio dense implant at the cortical defect of femoral epiphysis. The implanted material appeared to be radio dense and up to

mid medullary cavity. At day 30, radio dense implant was evidenced with similar density to that of host bone. The radio density was still unaltered at day 60 except reducing the size of the implant indicating moderate bone formation.

In 5% Zn- β-TCP group, at '0' day, the radiodense implant was evidenced at the defect of femoral epiphysis and merely reducing the length of implant at day 30 indicating mild degradation of implant and initiation of new bone formation. The implant was still visible radiodense to that of adjacent host tissue at day60 except moderate diminishing the size of the implant.

In 5% Mg- β-TCP group at day '0', the hyper dense implant was visible in the bone defect of femoral epiphysis and extended up to mid medullary cavity. At day 30 the size as well as the density of the implant was reduced as compared to earlier day. The size of the implant was further reduced indicating moderate degradation of implant and newly osseous tissue regeneration in the defect area.

In 5% Ti doped β-TCP implant group showed presence of well-placed radio dense implant in the bone defect of femoral epiphysis. At day 30, the radio density was still unaltered except significant reduction of the size of the implant indicating initiation of new bone formation. Subsequently at 60, the size of the implant was further reduced indicating degradation of the implant and more new bone formation in the defect site. The radiodensity was still visible.

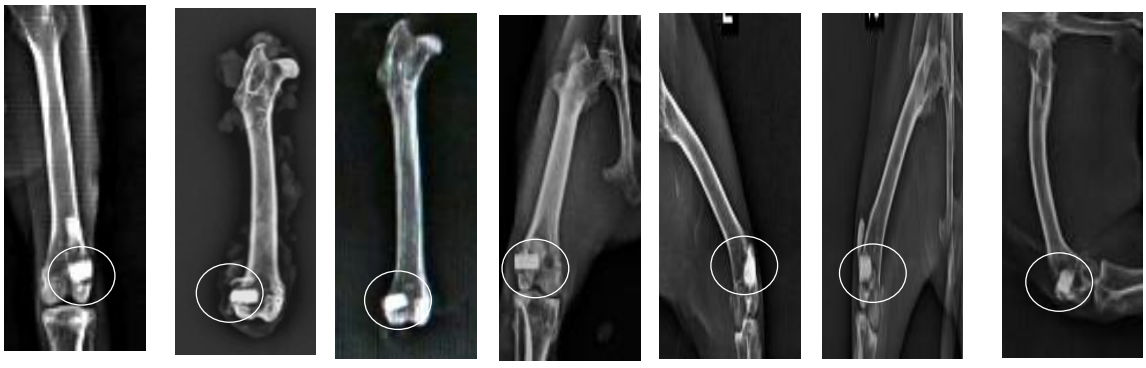

Figure 5.17: Radiographs of the '30' day
***NV: No Vibration (Group-II),**WV : With Vibration (Group-III)**

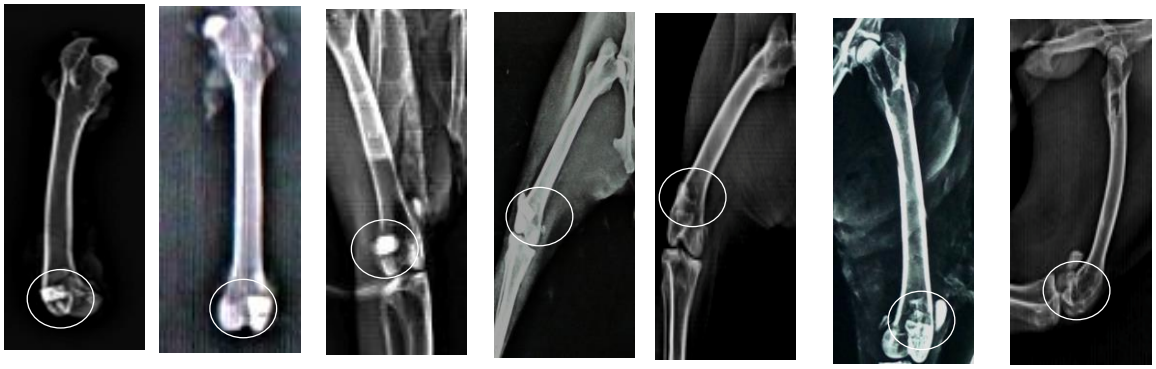

Control β-TCP- NV* Ti- β-TCP- NV β-TCP- WV** Ti- β-TCP- WV Mg- β-TCP- WV Zn β-TCP- WV

Figure.5.18: Radiographs of the '60' day
***NV: No Vibration (Group-II), **WV: With Vibration (Group-III)**

5.4.3 Micro-computed tomography

5.4.3.1a Control and test group II: Radiographic 2D images:

The Radiographic 2D images of defect bone sites with control and of pure β-TCP and Ti doped β-TCP after 1 M and 2 M are shown in Fig. 5.19. Which shows the healing as well as the bone regeneration inside the defect site. After two M, gradual degradation of the implant is seen and new bone regeneration was more prominent for Ti doped β-TCP compared to pure β-TCP and control.

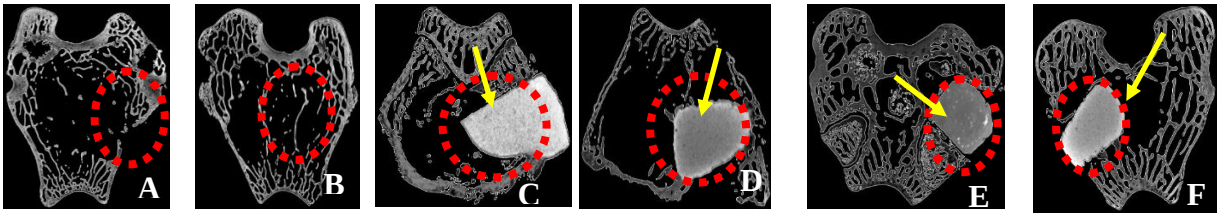

Figure 5.19: Radiographic 2D images of defect bone sites; with control: (A) 30 Days. (B) 60 Days. With β- TCP : (C) 30 Days. (D) 60 Days, with Ti -β-TCP: (E) 30 Days. (F) 60 Days (Red broken ring showing the defect site, Yellow arrow-Implant material)

5.4.3.1b Radiographic 3D images:

The 3D micrographs of bone implant interface of control, undoped and Ti doped β-TCP are shown in figure 5.20. After 1M, bone growth can be seen in both undoped and Ti doped implants showing the osteoconductive property of the TCP ceramics. The 2M images indicated that Ti

doped β-TCP showed gradual degradation of the ceramics and higher amount of bone formation around the implant. The degraded products are adsorbed and the resorption process was more for Ti doped β-TCP ceramics compared to undoped one resulting in the formation of thick struts of trabecular bone around the implant **(Fig.5.20).**

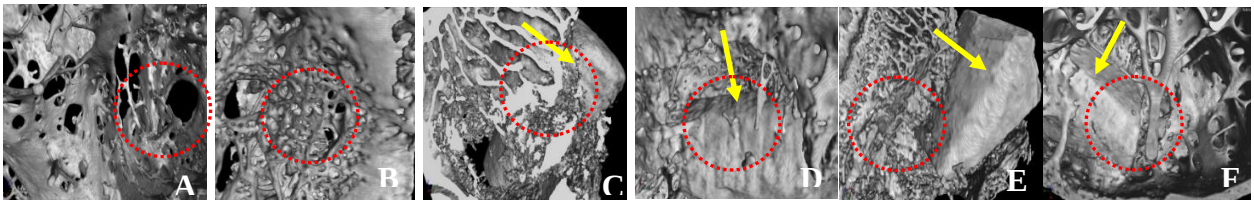

Figure 5.20: 3D micrographs of defect bone sites; with control: (A) 30 Days. (B) 60 Days. With β-TCP: (C) 30 Days. (D) 60 Days, with Ti- β-TCP: (E) 30 Days. (F) 60 Days
(Red broken ring showing the defect site, Yellow arrow-Implant material)

5.4.3.2a Test group III: Radiographic 2D images:

The in vivo micro-CT studies of rabbit femoral condyle indicated the growth of new bone regeneration by the degradation of implants and release of the dopants. Figure 5.21 shows the radiographic 2D images of defect bone sites, showing the healing of bone as well as the bone growth to the bone-material interface.

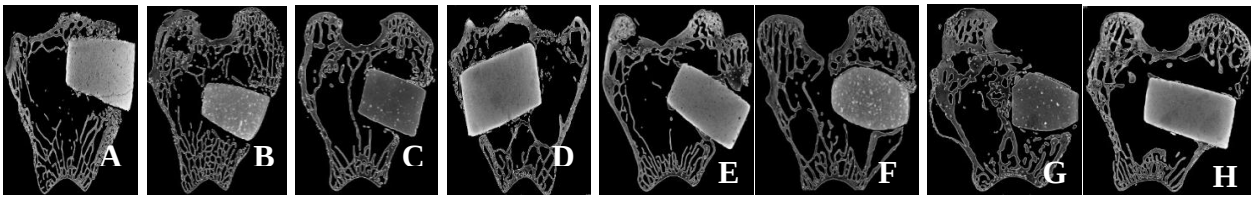

Figure 5.21: Radiographic 2D images of group III animal;1 M after installation: A. β-TCP, B. Zn- β-TCP, C. Mg- β-TCP, D. Ti- β-TCP and 2 M after installation: E. β-TCP, F. Zn- β-TCP, G. Mg- β-TCP, H. Ti- β-TCP

5.4.3.2b Test group III: Radiographic 3D images

The 1M post-implant 3D micro-CT images (Figure 5.22) showed that bone has started to grow on all the implants indicating the osteoconductive nature of the ceramics. The gradual degradation behaviour of the implant showed the irregularity in shape and among the other implants, Ti doped β-TCP showed a remarkable amount of newly formed bony tissue surrounding the implant. The 2M post-implant images has undergone remodelling, which is seen from their shape and structural stability. The resorption process was more pronounced for

Ti- β-TCP with thick newly formed bony tissue and large struts of trabecular bone were formed on the implant.

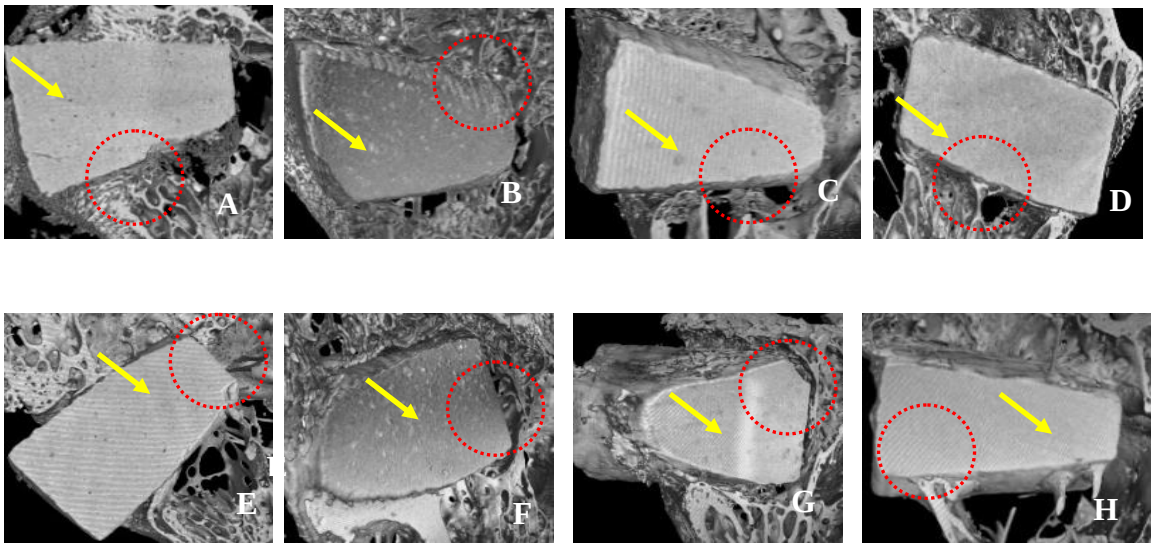

Figure 5.22: Radiographic 3D images of group III animal: 1 M after installation. A.β-TCP, B. Zn-β-TCP, C. Mg- β-TCP, D. Ti- β-TCP and 2 M after installation. E. β-TCP, F. Zn- β-TCP, G. Mg- β-TCP, H. Ti- β-TCP (Red broken ring showing the defect site, Yellow arrow-Implant material)

5.4.4 Histological study:

5.4.4a Control

Control 1 M sample picture depicted normal histology of bony structure containing numerous haversian canal (HC) with multiple lamellae. Medullary cavity contained few RBCs and mononuclear (MN) cells, scanty amount of fibrin and fewosteocyte.Angiogenesis is quite normal.Control 2 M sample section depicted normal histology of bony structure containing numerous haversian canal (HC) with multiple lamellae. Medullary cavity contained few RBCs and mononuclear (MN) cells, scanty amount of fibrin and scares osteocyte.Angiogenesis invasion was quite normal.The picture of this control sample is given in figure 5.23.

5.4.4b Group II

TCP 1M sample section depicted osseous bony matrix characterized by presence of bony spicules along with infiltration of mononuclear cell, osteoblast, and few osteoclasts. Angio-invasions are moderate. The medullary sinus contained scanty fibrinous deposit and few R.B.C's. The cortex of bony structures was invaded by fibroblastic tissue proliferation. β-TCP 2M section

showed presence of haversian canal with medullary sinuses. The bony plate was invaded by narrow sheets of osseous tissues containing osteoblasts along with fibroblastic proliferation. The medullary cavity contained RBCs, few osteocytes and fibrinous deposits.

Ti- β-TCP 2M section resembled a healthy osteogenic tissue containing abundant haversian canal and laminar plates. The medullary cavity contained fat cells, RBC's, osteoblast and few osteocytes. Ti- β-TCP 2M sample section showed bony structures with supporting stroma. The bony plate was invaded by abundant osteoclastic cell indicating massive regeneration and repair. The medullary cavity contained few fat cells, R.B.C's osteoblasts and few osteoclasts. Neo-osseous bone formation was found along with abundant angio-invasion indicating fair regenerative process. The picture of this group is given in figure 5.23.

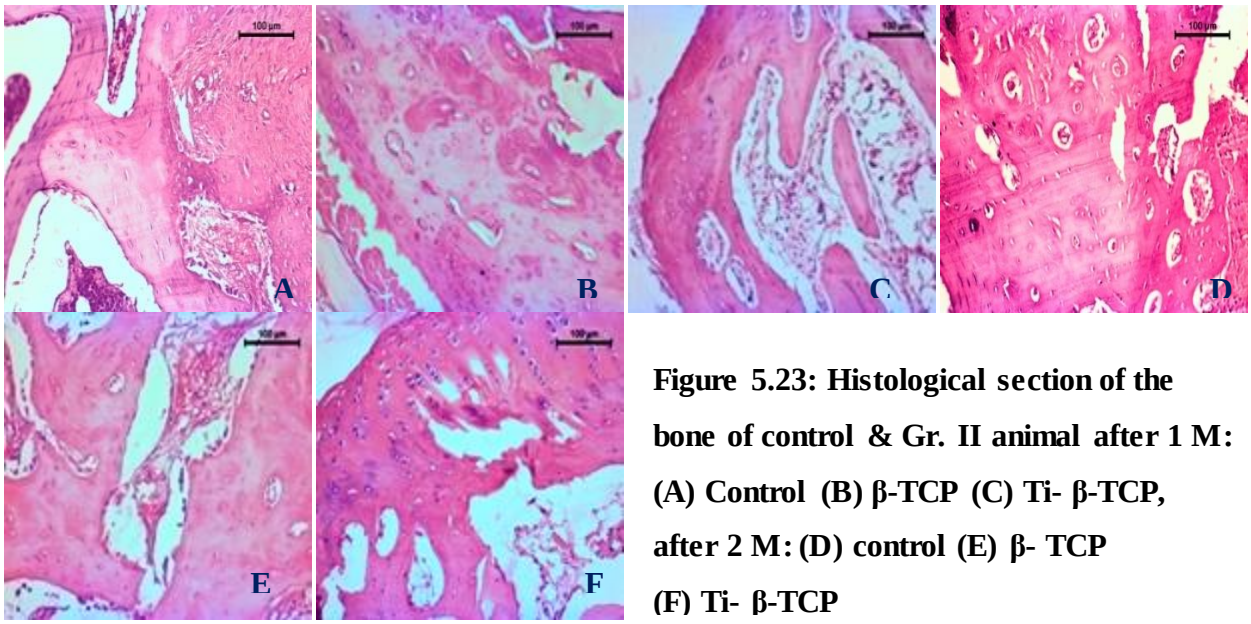

Figure 5.23: Histological section of the bone of control & Gr. II animal after 1 M: (A) Control (B) β-TCP (C) Ti- β-TCP, after 2 M: (D) control (E) β- TCP (F) Ti- β-TCP

5.4.4c Test group III

β-TCP 1M sample section showed bony osteoids containing bony lamellae and bony matrix proliferation with MN cells, few osteoclast and osteocytes.Medullary cavity contained scanty amount of RBCs, fibrin and mononuclear cells. Angio-invasion is moderately less.5%Zn β-TCP 1Msample section depicted a well-organized bony osteoid containing few osteoclast, osteocytes and rare amount of osteoblast. The medullary cavity was filled with RBCs, fibrin & mononuclear cells. The fibrovascular proliferation wasnormal.5% Mg β-TCP 1M sample section depicted well regenerated osteoids containing new HC, fibrovascular proliferation & sufficient angio invasion (figure 5.24).The bony matrix was infiltrated with few osteoblasts, osteoclast and scanty amount of osteocytes.5% Ti β-TCP 1M sample section depicted a good proliferating and

regenerating pictures of bony matrices, containing haversian canal, bony lamella in sufficient proportion, fibro-collagenous proliferation in proper manner. The angio-invasion are highly satisfactory and the fibrinous exudation in lamellar portion along with osteoblast, osteocytes indicating quick regeneration of bony tissue.

β-TCP 2M sample section depicted a newly formed bony matrix along with medullary portion containing sufficient amount of adipose tissues, mononuclear cells, RBCs and few fibrin deposit. The angio-invasion and fibrovascular proliferation were moderate.5% Zn β-TCP 2M sample section structure depicted a highly proliferated bony matrix containing numerous haversian canal, fibro-collagenous proliferation and sufficient amount of angiogenic points. The medullary cavity was filled with RBCs, few mononuclear cells and few osteoblasts.5% Mg β-TCP 2M sample section depicted a well regenerated bony matrix containing newly laid calcified matrix along with sufficient proliferation of vascular collagenous elements. The medullary cavity was filled with RBCs, fibrin & few osteocytes.5% Ti β-TCP 2M sample section depicted bony structure along satisfactorily regenerated tissue and characterized by sufficient fibro-vascularization, formation of sufficient angiogenic vessels and bony matrices containing few osteoclast, solitary osteoblast and osteocytes. The angiogenesis were quite normal.

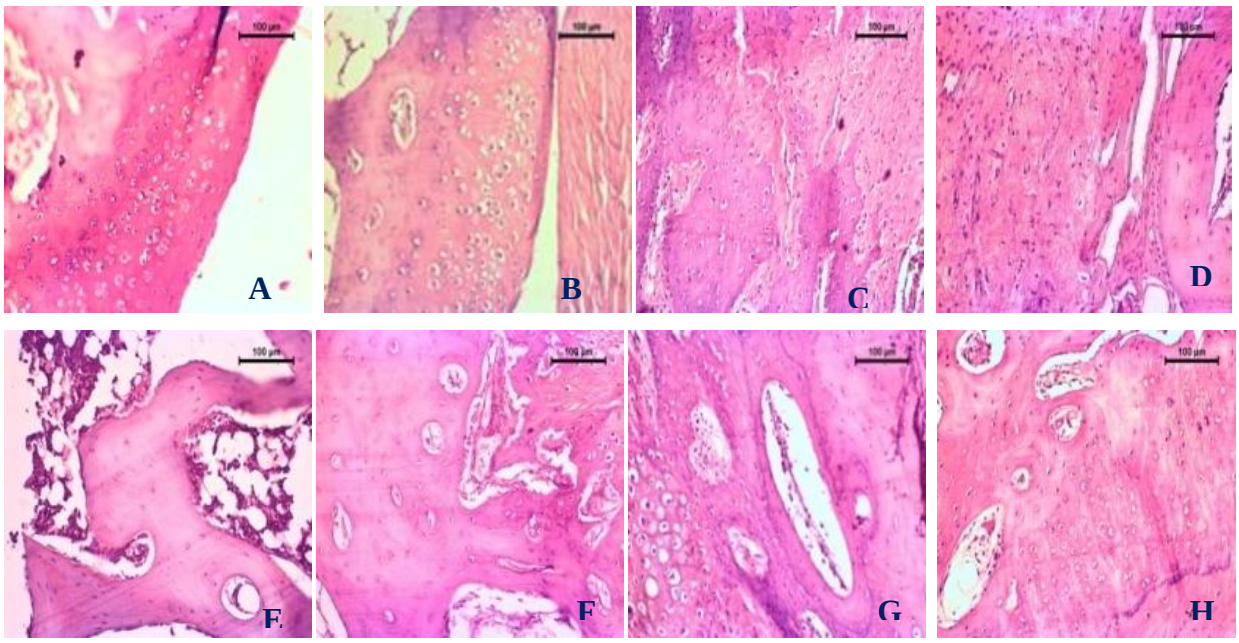

Figure 5.24: Histological section of the bone in group III after 1M of installation.A. β-TCP, B.Zn- β-TCP, C. Mg- β-TCP, D.Ti- β-TCP and after 2M of installation. E. β-TCP, F. Zn- β-TCP,G.Mg- β-TCP, H.Ti- β-TCP

5.4.5 Oxytetracycline labelling study

Oxytetracycline labelled new bone produced characteristic bright golden yellow fluorescence whilst host bone emitted sea green fluorescence under UV radiations. The implanted bone specimens were harvested at 1 and 2 M from each group. The pictures of both 1M and 2M specimens are given in the below figure 5.25.

5.4.5a Control: At 1 M, control sample showed mild bone formation (15.49± 2.97%) which increased with the passage of time at 2 M (22.28± 2.97%).

5.4.5b Test group II:

β-TCP sample section picture showed a narrow band of golden yellow fluorescence (19.56 ±3.07) in the center of bone specimen at 1M. The intensity of this golden yellow fluorescence (new osseous tissue) was further increased with time and mostly occupying centre to peripheral part. The amount of new bone formation was nearly 28.24 ± 3.04 % at 2M time point. In 1M Ti-β-TCP implanted bone samples showed patchy golden yellow fluorescence throughout the section and amount was nearly 29.56 ±1.72 %. At 2M time point, the intensity of golden yellow fluorescence was more as compared to 1 M time indicating more neo-osseous tissue formation at the defect area. At this stage, the amount was nearly 46.37 ±2.02 %.

5.4.5c Test group III:

At 1 M, β-TCP implanted bone specimens showed moderate new bone formation (26.96±3.97 %) whereas doped sample showed better performance of new bone formation at the same time point. It was observed that 5% Zn- β-TCP sample showed (34.62±4.03 %), 5% Mg- β-TCP of (38.21±1.97 %) and 5%Ti- β-TCP of (49.56±3.03 %) new bone formation as presence of golden yellow fluorescence. Comparatively more golden yellow fluorescence was observed at 2M in all doped samples. The amount of new bone formation was 34.46±3.02 %, 47.71±3.03 %, 48.35± 3.01% and 64.27±2.02 % in β-TCP,5% Zn- β-TCP, 5% Mg- β-TCP and 5%Ti- β-TCP bone samples respectively. The best new bone formation amongst the samples was observed in 5% Ti-β-TCP samples in the present study.

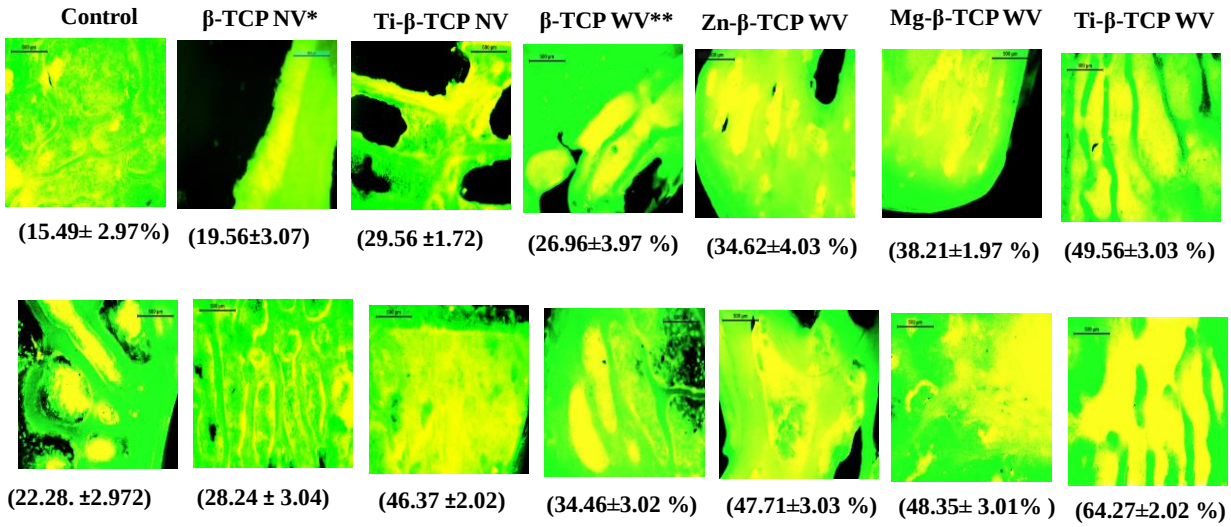

Figure 5.25: Oxytetracycline labeling study at the defected site of the group Control, Group II & Group III animal after 1M and 2M of installation. The yellow portions depict new bone formation

Table 5.10: Oxytetracycline labelling study result of % new bone formation in 1M & 2M

Composition	1M	SD (±)	2 M	SD (±)
Control	15.49	2.971	22.28	2.972
β-TCP NV*	19.56	3.07	28.24	3.040
β-TCP WV**	26.96	3.979	34.46	3.026
Ti-β-TCP NV	29.56	1.728	46.37	2.027
Ti-β-TCP WV	49.56	3.031	64.27	2.020
Zn-β-TCP WV	34.62	4.036	47.71	3.030
Mg-β-TCP WV	38.21	1.971	48.35	3.016

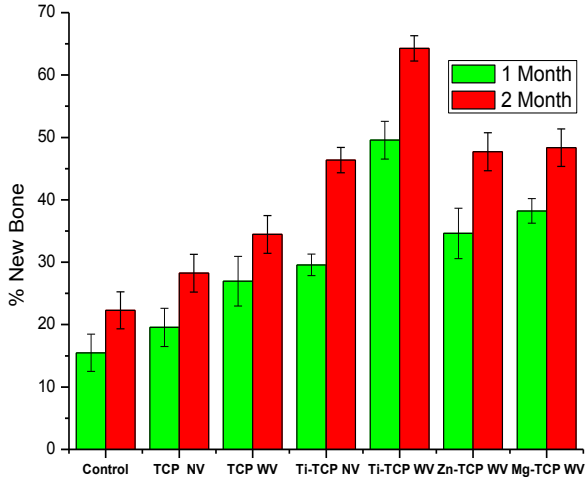

Figure 5.26: Bar diagram showing % new bone formation in 1 month and 2 Month. NV*: No Vibration, WV: With Vibration**

5.4.5 SEM images of Bone Implant Interface study:

The SEM images of control and Group II animals' bone-implant-interfaces (BII) of pure β-TCP and doped β-TCP ceramics have been analyzed using SEM and the images are shown in figure 5.27.

5.4.5a Control: The SEM images of the defect site show that the gap is quite visible in 1M and after 2M, a minor portion has been covered.

5.4.5b Test group II: After 1M, doped β-TCP showed some irregular bone tissue which can bind the implant and the old bone. The bridging gap between the implant and the native bone was found to be lesser for pure β-TCP compared to doped ceramics. At the end of 2M, Ti- β-TCP binds the entire bridging with new bone formation and holds the implant firmly proving that the implant has the bone binding properties.

5.4.5c Test group III: The SEM images of BII of undoped and doped TCP for 1M and 2M are shown in figure 5.27. The BII was carried out to study the bridging gap between the implant and bone by new bone formation. Pure β-TCP has not shown much integrated BII when compared to doped implants. With increasing in time from 1M to 2M, Zn and Mg dopant showed an irregular bony deposition that bonds the mature bone to hold the implant inside with new bone formation at the interface where as Ti- β-TCP resulted in stronger bone formation and gives a far better evidence of bone regeneration at the interface. At 2M Ti- β-TCP almost covers the entire bridging. The interfacial newly formed bone formation was indicative of the fact that the implant has sufficient bone binding properties.

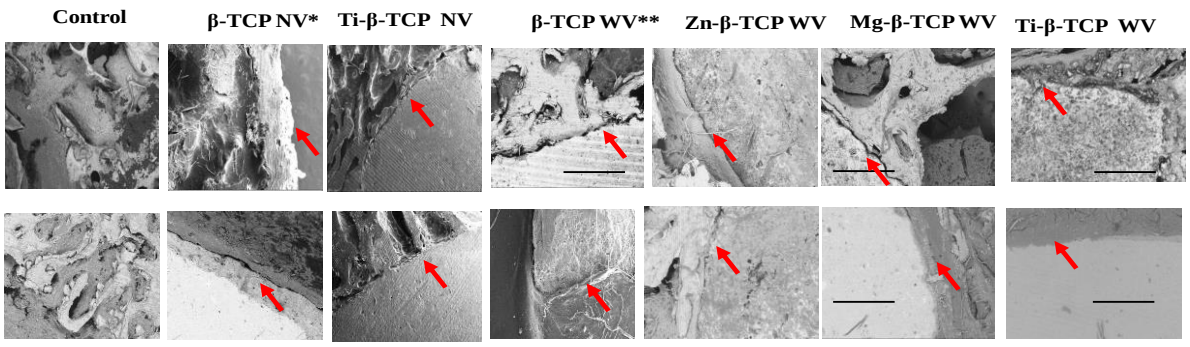

Figure 5.27: SEM images of all groups of bone implant interface after 1 Month & 2 Month (Red arrow-showing the interface between the bone and the implant. Scale bar =100µm)

Major Observations

- **No materials show any inflammatory reaction. All the implants were clinically stable in the bone.**
- **Radiograph taken at different animals revealed appreciable evidence of faster. healing for β-TCP and its doped compositions than Control group.**
- **Histopathological study depicted a good proliferating and regenerating pictures of bony matrices in all Group III animals compared to other groups.**
- **SEM images of bone implant interface showed some remarkable differences in different group of animals and with different compositions.**
- **The bonding of implant with host bone was better in Group III animals compared to other two groups.**
- **The oxytetracycline labelling study clearly showed the % of new bone formation was much better in Group III animals.**
- **In Group III animals the Ti doped implant gave the maximum % of new bone formation.**

This study confirmed that the quantity of new bone formation is much more in case of 5% Ti-β- under axial oscillatory vibration as compared to pure β-TCP(under both group II & group III) , 5%Zn-β-TCP (group III), 5%Mg-β-TCP (group III) and control group of animals. In general, the doped samples showed significantly better bone regeneration with cyclic loading conditions than pure β-TCP specimens. This proves that loading effect simalteneously with doping agent have marked influence on bone regeneration. The possible reasons behind this positive effete may be attributed to many different reasons as described by many researchers.

One possible reason could be the piezoelectricity theory [Fakuda and Yasuda 1950] .According to that bone modulates its structure by sensing mechanical stresses generated by dynamic loading and unloading cycles in vivo which in turn generate the electricity that triggers the remodeling activities.

Another possible reason is strain generated potentials(SGPs).It is conceivable that more rigorous activities on bone will lead to higher kinetic activities of ions which will induce higher streaming potentials which, in turn will signal more bone mineral deposition[3]. The other aspects of fast remodeling of bone in response to loading is achieved via mechanotransduction, a process through which forces or other mechanical signals are converted to biochemical signals in cellular signaling [4]. Mechanotransduction leading to bone remodeling involve the steps of mechanocoupling, biochemical coupling, signal transmission, and cell response[5] .The specific effects on bone structure depends on the duration, magnitude and rate of loading, and it has been found that only cyclic loading can induce bone formation[5]. When loaded, fluid flows away from areas of high compressive loading in the bone matrix [6]. Osteocytes have been hypothesized to be the major mechanosensors in bone [7]. Osteocytes can extend their dendritic processes to communicate with osteoblasts and possibly osteoclasts on the bone surface and regulate the matrix remodeling activities of these cells through factors such as receptor activator of nuclear factor-$_{k}$B ligand (RANKL) and sclerostin [8,9]. The osteocyte network has been hypothesized to be the central mechanosensor that orchestrates bone modeling and remodeling by detecting mechanical stimuli applied to the skeleton [10] through interstitial fluid flow [11].

Upon sensing a load, osteocytes regulate bone remodeling by signaling to other cells with signaling molecules or direct contact [12]. Additionally, osteoprogenitor cells, which may differentiate into osteoblasts or osteoclasts, are also mechanosensors and may differentiate one

way or another depending on the loading condition.[12] Osteoclasts and osteoblasts arrange themselves into temporary anatomical structures called BMUs (basic multicellular units) that execute bone remodeling. BMUs are characterized by teams of osteoclasts that resorb bone in the characteristic "cutting cone" leading edge of the structure, followed by osteoblasts, which line the "closing cone" and centripetally deposit layers of new bone to refill the tunnel excavated by the osteoclasts. The new bone begins as unmineralized matrix (osteoid) [13].Another theory behind this effect is the displacement of cell nuclei. Vibrations can cause larger displacements in cell nuclei than fluid shear, indicating the mechanism of action is more likely due to the mechanical coupling between these oscillating cell nuclei and the cytoskeleton, which ultimately induces actin remodeling and reduces bone resorption [14, 15].We have observed here the better bone formation is shown by doped compositions. All the dopant ions are responsible for adding some additional electrical charge in the bone matrix. The dopant materials for this study are having some considerable dielectric constant. Titanium has an enormous high dielectric constant and can hold the charge for a longer period. As loading causes a local electrical callus [16] formation in the applied zone, presence of such dopant ions can create a localized potential difference and which can ultimately invite more fluid flow/blood flow to the affected portion to maintain the electrical neutrality and ultimately promotes better bone regeneration.

In continuity with the above mentioned discussion, it may be noted that two things simultaneously took place in this case, one is effect of doping and the other is mechanical loading in the form of vibration. The combined effect as evident from micro CT and other parameters clearly reveals that the benefits of doping (which is already accepted through large number of literature in last few decades) can be extended further by mechanical stimuli in the form of vibration. The combined effect of doping and vibration really enhanced the extent of new bone formation, may be through more effective mechano-transduction due to presence of metallic ions, (known to have positive effect on bone remodeling) however the exact micro-level intricacies are yet to be understood in a comprehensive way.

References

[1] Liu Ying, Wang Xiuping, Zhou Defeng, Ning Dezheng, Zhang Guanming, Meng Jian ,Effect of ZnO addition on the sintering and electrical properties of ceria-based electrolyte materials, advances in energy engineering (AEE) Volume 2, 2014

[2] Hoffler, C. E. (2005). An application of nanoindentation technique to measure bone tissue lamellae properties. Journal of Biomechanical Engineering, 127(7), 1046.

[3]J.B Park, Biomaterials Science and Engineering ,Plenum Press, NY & London

[4] Huang, Chenyu; Rei Ogawa. "Mechanotransduction in bone repair and regeneration". FASEB J. 24. Oct. 2010.

[5] Duncan, RL; CH Turner, Mechanotransduction and the functional response of bone to mechanical strain, Calcified Tissue International. 57 (5): 344–358. 1995

[6] Turner, CH; MR Forwood; MW Otter, Mechanotransduction in bone: do bone cells act as sensors of fluid flow?. FASEB J. 8 (11),1994.

[7] Da Jing, Andrew D. Baik X. Lucas Lu, Bin Zhou, Xiaohan Lai, Liyun Wang, Erping Luo, and X. Edward Guo,In situ intracellular calcium oscillations in osteocytes in intact mouse long bones under dynamic mechanical loading The FASEB Journal.

[8] Nakashima, T., Hayashi, M., Fukunaga, T., Kurata, K., Oh-Hora, M., Feng, J. Q., Bonewald, L. F., Kodama, T., Wutz, A., Wagner, E. F., Penninger, J. M., and Takayanagi, H. Evidence for osteocyte regulation of bone homeostasis through RANKL expression. Nat. Med. 17, 1231–1234, 2011.

[9] Moriishi, T., Fukuyama, R., Ito, M., Miyazaki, T., Maeno, T., Kawai, Y., Komori, H., and Komori, T. Osteocyte network; a negative regulatory system for bone mass augmented by the induction of Rankl in osteoblasts and Sost in osteocytes at unloading. PLoS One7,e40143,2012 .

[10] Turner, C. H., Robling, A. G., Duncan, R. L., and Burr, D. B. Do bone cells behave like a neuronal network? Calcif. Tissue Int. 70, 435–442, 2002.

[11] Fritton, S. P., and Weinbaum, S. Fluid and solute transport in bone: flow-induced mechanotransduction. Annu. Rev. Fluid Mech. 41, 347–374, 2009.

[12] Chen, Jan-Hung; Chao Liu; Lidan You; Craig A Simmons ,Boning up on Wolff's Law: Mechanical regulation of the cells that make and maintain bone. Journal of Biomechanics. 43: 108–118, 2010.

[13] Biomechanical and Molecular Regulation of Bone Remodeling Alexander G. Robling,1 Alesha B. Castillo,1,2 and Charles H. Turner2,3, Annu. Rev. Biomed. Eng.. 8:455–98, 2006.

[14] Lau E. AL-D S, Gunther A et al, Effect of low magnitude high frequency vibration on osteocyte in the regulation of osteoclast, Bone,46,1508-1515,2016.

[15] Uzer G,T WR,Sen B et al,Gap junctional communication in osteocytes is amplified by low intensity vibration in vitro ,PloS ONE,2014,9:90840 .

[16] C.T.Brighton, Z.B.Friedenberg and J.Black,Evaluation of the use of constant direct current in the treatment of nonunion,in :Electrical properties of Bone and cartilage,C.T.Brighton, J.Black and S .R. Pollack(ed.),pp.519-545,Grune & Stratton, New York,1979.

CHAPTER: 6

CONCLUSION & FUTURE SCOPE

Conclusion

In this work, we have prepared phase pure β-TCP and 3wt% and 5 wt %Zn, Mg and Ti doped β-TCP powders using chemical route method. In XRD study, we have got β-TCP phase in all compositions of doped and pure powder. The lattice parameters show that there is a direct shortening of length of the axis due to the reduction of atomic radius in different compositions. We have got uniform pattern of shrinkage in pure β-TCP and in all compositions of doped β-TCP powder in different sintering temperature. Porosity is greatly reduced with the increase of temperature. The concentration variation of dopants does not alter any kind of significant changes in grain size, porosity and in crystal structure. Good amount of porosity is present in all compositions which can promote anchorage of bone cells and bony in-growth. The hardness study results clearly indicate that there is little bit change of hardness due the addition of dopants .But there is no direct proportionate relation between the hardness and dopants amount. Contact angle of all samples clearly indicate that all the samples are truly hydrophilic. All the samples are hemocompatible as well as they are all nontoxic. SBF study indicates that the titanium doped variant is better than other varieties as it gives maximum apatite layer formation.

In light of the present results, it can be concluded that low frequency axial vibration, combined with metal ion doping, had a prominent effect on new bone formation. The study confirmed that the quantity of new bone formation is much more in case of 5%Ti-β-TCP as compared to (5% Zn-β-TCP, 5% Mg-β-TCP) and control group of animals. It may be attributed to the pronounced effect of Ti ion on promoting osteogenesis. In general, the doped samples showed significantly better bone regeneration with cyclic loading conditions than pure TCP specimens. From the detailed animal studies involving micro-CT, SEM etc, it may be concluded that external loading in the form of low frequency intermittent axial vibration with porous tricalcium phosphate (both pure and doped) based implants stimulates prompt new bone formation and presents an exciting possibility for orthopedic reconstructive procedures. However, further detailed studies are necessary to ascertain the exact reason behind the effect of dynamic loading on new bone regeneration.

Scope of the future work

1) Alternative bone substitutes can be taken in to the consideration.
2) Different frequency level can be tried for loading.
3) Frequency level can be increased weekly.
4) Time span of application can be altered.
5) *In- vivo* study in other model can be tried.
6) Clinical study can be done if ethical committee permits.